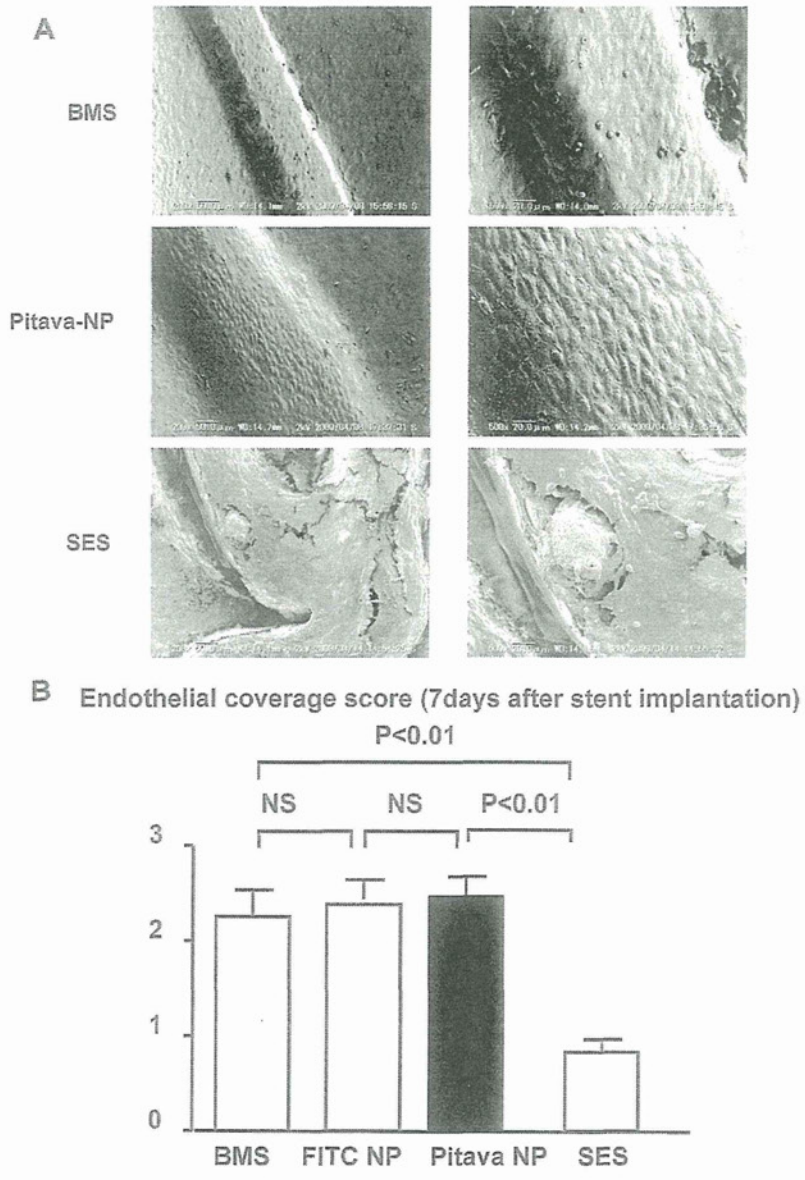

Fig. 7. Endothelial surface coverage analysis by scanning electron microscopy.

A, Representative micrographs of the endothelial surface by scanning electron microscopy one week after stent implantation. B, Endothelial coverage score one week after stent implantation in bare metal stent (BMS), FITC-NP-eluting stent (FITC-NP), pitavastatin-NP-eluting stent (Pitava-NP) stent, and sirolimus-eluting stent (SES) groups ($n=3$ each).

by impaired re-endothelialization and persistence of fibrin and inflammation are an important histopathological feature in arteries exposed to currently marketed DESs in experimental animals[33, 34] and in humans[4-6]. These delayed endothelial healing effects are presumed to result from the effects of drugs coated on DESs (see Introduction). Using human pathological data from autopsy patients in whom death occurred >30 days after drug-eluting stent placement, Finn *et al.*[6] demonstrated that endothelialization of the stent was the best predictor of late in-stent thrombosis. Heterogeneity of healing is a common finding in cases of late drug-eluting stent thrombosis. In this study, we confirmed the delayed endothelial healing effects of sirolimus-eluting stents in porcine coronary arteries (**Fig. 5**, 6, and 7) reported by Virmani's group[5]; however, we found that pitavastatin-NP-eluting stents had no such delayed endothelial healing effects in porcine coronary

arteries *in vivo*. The opposing effects of pitavastatin-NP-eluting stents and sirolimus-eluting stents might be explained by our *in vitro* study (**Fig. 1** and **2**). Collectively, these data on anti-endothelial healing properties suggest that pitavastatin-NP-eluting stents may have an advantage over currently marketed polymeric DES devices. Future studies are needed to prove this point.

A major limitation of this study is that this study was performed in normal pigs without pre-existing atherosclerotic coronary lesions, although this porcine coronary artery model is regarded as an appropriate and standard preclinical study model[35]. A long-term efficacy study is also needed.

In conclusion, pitavastatin-NP-eluting stents not only attenuated in-stent stenosis as effectively as polymer-coated sirolimus-eluting stents but also elicited endothelial healing effects in a porcine coronary artery model. Delayed endothelial healing is a common feature at atherosclerotic arterial sites deployed with currently marketed DESs, which may lead to an increased risk of late stent thrombosis. Our present technology can be one approach to overcome the adverse effects of current DESs and may provide the optimal anti-healing combination: the inhibition of VSMC proliferation to decrease restenosis and the promotion of re-endothelialization to protect from late stent thrombosis. This NP-eluting stent system may be developed as an innovative platform for the future treatment of atherosclerotic vascular disease.

Acknowledgments

Funding Sources: This study was supported by Grants-in-Aid for Scientific Research (19390216, 19650134) from the Ministry of Education, Science, and Culture, Tokyo, Japan, by Health Science Research Grants (Research on Translational Research and Nanomedicine) from the Ministry of Health Labor and Welfare, Tokyo, Japan, and by a Special Grant from Terumo Life Science Foundation, Tokyo, Japan.

Conflict of Interest

Dr. Egashira holds a patent on the results reported in the present study. The remaining authors report no conflicts.

References

1) Laskey WK, Yancy CW, Maisel WH: Thrombosis in coronary drug-eluting stents: Report from the meeting of the circulatory system medical devices advisory panel of the food and drug administration center for devices and radiologic health, december 7-8, 2006. Circulation, 2007; 115: 2352-2357
2) Serruys PW, Kutryk MJ, Ong AT: Coronary-artery stents. N Engl J Med, 2006; 354: 483-495
3) Shuchman M: Trading restenosis for thrombosis? New questions about drug-eluting stents. N Engl J Med, 2006; 355: 1949-1952
4) Luscher TF, Steffel J, Eberli FR, Joner M, Nakazawa G, Tanner FC, Virmani R: Drug-eluting stent and coronary thrombosis: Biological mechanisms and clinical implications. Circulation, 2007; 115: 1051-1058
5) Finn AV, Nakazawa G, Joner M, Kolodgie FD, Mont EK, Gold HK, Virmani R: Vascular responses to drug eluting stents. Importance of delayed healing. Arterioscler Thromb Vasc Biol, 2007; 27: 1500-1510
6) Finn AV, Joner M, Nakazawa G, Kolodgie F, Newell J, John MC, Gold HK, Virmani R: Pathological correlates of late drug-eluting stent thrombosis: Strut coverage as a marker of endothelialization. Circulation, 2007; 115: 2435-2441
7) Joner M, Nakazawa G, Finn AV, Quee SC, Coleman L, Acampado E, Wilson PS, Skorija K, Cheng Q, Xu X, Gold HK, Kolodgie FD, Virmani R: Endothelial cell recovery between comparator polymer-based drug-eluting stents. J Am Coll Cardiol, 2008; 52: 333-342
8) Takemoto M, Liao JK: Pleiotropic effects of 3-hydroxy-3-methylglutaryl coenzyme a reductase inhibitors. Arterioscler Thromb Vasc Biol, 2001; 21: 1712-1719
9) Eto M, Kozai T, Cosentino F, Joch H, Luscher TF: Statin prevents tissue factor expression in human endothelial cells: Role of rho/rho-kinase and akt pathways. Circulation, 2002; 105: 1756-1759
10) Thyberg J: Re-endothelialization via bone marrow-derived progenitor cells: Still another target of statins in vascular disease. Arterioscler Thromb Vasc Biol, 2002; 22: 1509-1511
11) Werner N, Priller J, Laufs U, Endres M, Bohm M, Dirnagl U, Nickenig G: Bone marrow-derived progenitor cells modulate vascular reendothelialization and neointimal formation: Effect of 3-hydroxy-3-methylglutaryl coenzyme a reductase inhibition. Arterioscler Thromb Vasc Biol, 2002; 22: 1567-1572
12) Yokoyama T, Miyauchi K, Kurata T, Satoh H, Daida H: Inhibitory efficacy of pitavastatin on the early inflammatory response and neointimal thickening in a porcine coronary after stenting. Atherosclerosis, 2004; 174: 253-259
13) Indolfi C, Cioppa A, Stabile E, Di Lorenzo E, Esposito G, Pisani A, Leccia A, Cavuto L, Stingone AM, Chieffo A, Capozzolo C, Chiariello M: Effects of hydroxymethylglutaryl coenzyme a reductase inhibitor simvastatin on smooth muscle cell proliferation in vitro and neointimal formation in vivo after vascular injury. J Am Coll Cardiol, 2000; 35: 214-221
14) Scheller B, Schmitt A, Bohm M, Nickenig G: Atorvastatin stent coating does not reduce neointimal proliferation after coronary stenting. Zeitschrift fur Kardiologie, 2003; 92: 1025-1028
15) Miyauchi K, Kasai T, Yokayama T, Aihara K, Kurata T, Kajimoto K, Okazaki S, Ishiyama H, Daida H: Effectiveness of statin-eluting stent on early inflammatory response

and neointimal thickness in a porcine coronary model. Circ J, 2008; 72: 832-838
16) Serruys PW, Foley DP, Jackson G, Bonnier H, Macaya C, Vrolix M, Branzi A, Shepherd J, Suryapranata H, de Feyter PJ, Melkert R, van Es GA, Pfister PJ: A randomized placebo-controlled trial of fluvastatin for prevention of restenosis after successful coronary balloon angioplasty; final results of the fluvastatin angiographic restenosis (flare) trial. Eur Heart J, 1999; 20: 58-69
17) Bertrand ME, McFadden EP, Fruchart JC, Van Belle E, Commeau P, Grollier G, Bassand JP, Machecourt J, Cassagnes J, Mossard JM, Vacheron A, Castaigne A, Danchin N, Lablanche JM: Effect of pravastatin on angiographic restenosis after coronary balloon angioplasty. The predict trial investigators. Prevention of restenosis by elisor after transluminal coronary angioplasty. J Am Coll Cardiol, 1997; 30: 863-869
18) Weintraub WS, Boccuzzi SJ, Klein JL, Kosinski AS, King SB, 3rd, Ivanhoe R, Cedarholm JC, Stillabower ME, Talley JD, DeMaio SJ, et al: Lack of effect of lovastatin on restenosis after coronary angioplasty. Lovastatin restenosis trial study group. N Engl J Med, 1994; 331: 1331-1337
19) Onaka H, Hirota Y, Kita Y, Tsuji R, Ishii K, Ishimura T, Kawamura K: The effect of pravastatin on prevention of restenosis after successful percutaneous transluminal coronary angioplasty. Jpn Circ J, 1994; 58: 100-106
20) Bae JH, Bassenge E, Kim KY, Synn YC, Park KR, Schwemmer M: Effects of low-dose atorvastatin on vascular responses in patients undergoing percutaneous coronary intervention with stenting. J Cardiovasc Pharmacol Ther, 2004; 9: 185-192
21) Petronio AS, Amoroso G, Limbruno U, Papini B, De Carlo M, Micheli A, Ciabatti N, Mariani M: Simvastatin does not inhibit intimal hyperplasia and restenosis but promotes plaque regression in normocholesterolemic patients undergoing coronary stenting: A randomized study with intravascular ultrasound. Am Heart J, 2005; 149: 520-526
22) Nakano K, Egashira K, Masuda S, Funakoshi K, Zhao G, Kimura S, Matoba T, Sueishi K, Endo Y, Kawashima Y, Hara K, Tsujimoto H, Tominaga R, Sunagawa K: Formulation of nanoparticle-eluting stents by a cationic electrodeposition coating technology efficient nano-drug delivery via bioabsorbable polymeric nanoparticle-eluting stents in porcine coronary arteries. JACC Cardiovasc Interv, 2009; 2: 277-283
23) Kimura S, Egashira K, Nakano K, Iwata E, Miyagawa M, Tsujimoto H, Hara K, Kawashima Y, Tominaga R, Sunagawa K: Local delivery of imatinib mesylate (sti571)-incorporated nanoparticle ex vivo suppresses vein graft neointima formation. Circulation, 2008; 118: S65-70
24) Masuda S, Nakano K, Funakoshi K, Zhao G, Meng W, Kimura S, Matoba T, Miyagawa M, Iwata E, Sunagawa K, Egashira K: Imatinib mesylate-incorporated nanoparticle-eluting stent attenuates in-stent neointimal formation in porcine coronary arteries. J Atheroscler Thromb, 2011; 18: 1043-1053
25) Aoki T, Nishimura H, Nakagawa S, Kojima J, Suzuki H, Tamaki T, Wada Y, Yokoo N, Sato F, Kimata H, Kitahara M, Toyoda K, Sakashita M, Saito Y: Pharmacological profile of a novel synthetic inhibitor of 3-hydroxy-3-methylglutaryl-coenzyme a reductase. Arzneimittel-Forschung, 1997; 47: 904-909
26) Ohtani K, Usui M, Nakano K, Kohjimoto Y, Kitajima S, Hirouchi Y, Li XH, Kitamoto S, Takeshita A, Egashira K: Antimonocyte chemoattractant protein-1 gene therapy reduces experimental in-stent restenosis in hypercholesterolemic rabbits and monkeys. Gene Ther, 2004; 11: 1273-1282
27) Camici GG, Steffel J, Akhmedov A, Schafer N, Baldinger J, Schulz U, Shojaati K, Matter CM, Yang Z, Luscher TF, Tanner FC: Dimethyl sulfoxide inhibits tissue factor expression, thrombus formation, and vascular smooth muscle cell activation: A potential treatment strategy for drug-eluting stents. Circulation, 2006; 114: 1512-1521
28) Egashira K, Nakano K, Ohtani K, Funakoshi K, Zhao G, Ihara Y, Koga J, Kimura S, Tominaga R, Sunagawa K: Local delivery of anti-monocyte chemoattractant protein-1 by gene-eluting stents attenuates in-stent stenosis in rabbits and monkeys. Arterioscler Thromb Vasc Biol, 2007; 27: 2563-2568
29) Usui M, Egashira K, Ohtani K, Kataoka C, Ishibashi M, Hiasa K, Katoh M, Zhao Q, Kitamoto S, Takeshita A: Anti-monocyte chemoattractant protein-1 gene therapy inhibits restenotic changes (neointimal hyperplasia) after balloon injury in rats and monkeys. FASEB J, 2002; 16: 1838-1840
30) Egashira K, Zhao Q, Kataoka C, Ohtani K, Usui M, Charo IF, Nishida K, Inoue S, Katoh M, Ichiki T, Takeshita A: Importance of monocyte chemoattractant protein-1 pathway in neointimal hyperplasia after periarterial injury in mice and monkeys. Circ Res, 2002; 90: 1167-1172
31) Egashira K: Molecular mechanisms mediating inflammation in vascular disease: Special reference to monocyte chemoattractant protein-1. Hypertension, 2003; 41: 834-841
32) Ohtani K, Egashira K, Nakano K, Zhao G, Funakoshi K, Ihara Y, Kimura S, Tominaga R, Morishita R, Sunagawa K: Stent-based local delivery of nuclear factor-kappab decoy attenuates in-stent restenosis in hypercholesterolemic rabbits. Circulation, 2006; 114: 2773-2779
33) van der Giessen WJ, Lincoff AM, Schwartz RS, van Beusekom HM, Serruys PW, Holmes DR Jr, Ellis SG, Topol EJ: Marked inflammatory sequelae to implantation of biodegradable and nonbiodegradable polymers in porcine coronary arteries. Circulation, 1996; 94: 1690-1697
34) Lincoff AM, Furst JG, Ellis SG, Tuch RJ, Topol EJ: Sustained local delivery of dexamethasone by a novel intravascular eluting stent to prevent restenosis in the porcine coronary injury model. J Am Coll Cardiol, 1997; 29: 808-816
35) Schwartz RS, Edelman ER, Carter A, Chronos N, Rogers C, Robinson KA, Waksman R, Weinberger J, Wilensky RL, Jensen DN, Zuckerman BD, Virmani R: Drug-eluting stents in preclinical studies: Recommended evaluation from a consensus group. Circulation, 2002; 106: 1867-1873

Circulation Journal
Official Journal of the Japanese Circulation Society
http://www.j-circ.or.jp

ORIGINAL ARTICLE
Myocardial Disease

Exercise-Induced ST Elevation in Patients With Non-Ischemic Dilated Cardiomyopathy and Narrow QRS Complexes

– Novel Predictor of Long-Term Prognosis From Exercise Testing –

Hiroyuki Takahama, MD; Hiroshi Takaki, MD; Yusuke Sata, MD; Kazushi Sakane, MD; Yasushi Ino, MD; Teruo Noguchi, MD; Yoichi Goto, MD; Masaru Sugimachi, MD

Background: The clinical significance and prevalence of exercise-induced ST elevation (ESTE) in non-ischemic dilated cardiomyopathy (NIDCM) patients are unknown.

Methods and Results: We retrospectively examined 12-lead ECGs during cardiopulmonary exercise testing in 360 consecutive NIDCM patients (left ventricular ejection fraction (LVEF) <45%) with narrow QRS. ESTE was defined as ≥1.0 mm ST (J-point) elevation compared with baseline. During long-term follow-up for major cardiac events (death, transplantation, or LV assist device implantation), ESTE was recognized in 50 patients (14%). They had much lower LVEF than patients without ESTE (20±7% vs. 27±7%, respectively, P<0.001), whereas the differences in peak $\dot{V}O_2$ (P=0.01) and $\dot{V}E/\dot{V}CO_2$ slope (P=0.04) were relatively small. Major cardiac events occurred more frequently in patients with ESTE than in those without ESTE (39% vs. 12% at 48 months). Increased event rates were associated with low peak $\dot{V}O_2$ (<14 ml·min^{-1}·kg^{-1}) in patients without ESTE (39% vs. 23%, P<0.05), but not in those with ESTE (50% vs. 62%, NS). Cox multivariate analysis revealed ESTE as the strongest independent prognosticator among exercise parameters (hazard ratio: 2.41 [95% confidence interval 1.03–5.63], P<0.05).

Conclusions: A substantial number of NIDCM patients exhibit ESTE, which indicates a poor prognosis. Low peak $\dot{V}O_2$ and ESTE may reflect different aspects of the pathophysiological processes that deteriorate heart failure. (*Circ J* 2013; **77:** 1033–1039)

Key Words: Cardiomyopathy; Electrophysiology; Exercise

Non-ischemic dilated cardiomyopathy (NIDCM) refers to a spectrum of heterogeneous myocardial disorders that are characterized by diffuse left ventricular (LV) dysfunction causing heart failure (HF) in the absence of coronary artery lesions, although the responsible mechanisms have not been completely clarified.[1–3] Despite remarkable recent advances in the treatment for HF, the prognosis remains poor for patients with NIDCM, as well as those with ischemic DCM. Furthermore, in countries such as Japan where coronary artery disease is less prevalent than in Western countries, the vast majority of middle-aged or young adult patients with advanced HF who are candidates for heart transplantation suffer from NIDCM.[4,5] Therefore, there is a pressing need to accurately identify the patients with NIDCM who are at high risk.

Exercise testing is an important clinical tool for this purpose, especially when coupled with respiratory gas exchange analysis (cardiopulmonary exercise testing: CPET). Although CPET provides established prognostic markers, such as peak oxygen uptake ($\dot{V}O_2$) and the regression slope relating minute ventilation to carbon dioxide output ($\dot{V}E/\dot{V}CO_2$ slope),[6,7] gas analysis is not performed in many hospitals. The standard 12-lead ECG, which is routinely recorded during exercise testing regardless, with or without gas analysis, is utilized almost exclusively for monitoring cardiac rhythm and myocardial ischemia; however, additional information for evaluating HF patients may be obtained from ECG. One such parameter would be exercise-induced ST-segment elevation (ESTE). ESTE is observed most commonly in the Q-wave leads in patients with prior myocardial infarction (MI), which is classically considered as representing severe wall motion abnormalities of the LV.[8–13] Because our previous study examining patients with arrhythmogenic right ventricular cardiomyopathy[14] indicated that ESTE was

Received June 22, 2012; revised manuscript received October 11, 2012; accepted November 16, 2012; released online December 29, 2012 Time for primary review: 25 days

Department of Cardiovascular Medicine, National Cerebral and Cardiovascular Center, Suita (H. Takahama, K.S., Y.I., T.N., Y.G.); Department of Cardiovascular Dynamics, National Cerebral and Cardiovascular Center Research Institute (H. Takaki, Y.S., M.S.), Suita, Japan
Mailing address: Hiroshi Takaki, MD, Department of Cardiovascular Dynamics, National Cerebral and Cardiovascular Center Research Institute, 5-7-1 Fujishirodai, Suita 565-8565, Japan. E-mail: htakaki@ri.ncvc.go.jp

ISSN-1346-9843 doi:10.1253/circj.CJ-12-0814

Table 1. Clinical Characteristics of Patients With Non-Ischemic Dilated Cardiomyopathy and Narrow QRS Complexes

n	360
Age (years)	48±15
Sex (M/F)	289/71
NYHA	2.1±0.7
LVEF (%)	26±8
LVDd (mm)	65±9
LVDs (mm)	54±11
Exercise time (s)	468±138
Peak work rate (W)	116±38
Peak SBP (mmHg)	156±37
Peak $\dot{V}O_2$ ($ml \cdot min^{-1} \cdot kg^{-1}$)	20.4±5.2
$\dot{V}E/\dot{V}CO_2$ slope	30±7
Peak RER	1.26±0.13

Values are mean±SD.
LVEF, left ventricular ejection fraction; LVDd, left ventricular end-diastolic dimension; LVDs, left ventricular end-systolic dimension; NYHA, New York Heart Association; Peak SBP, peak systolic blood pressure; RER, repiratory exchange ratio; $\dot{V}E/\dot{V}CO_2$ slope, regression slope relating minute ventilation to carbon dioxide output; $\dot{V}O_2$, oxygen uptake.

found to be closely associated with severe wall motion abnormalities of the right ventricle, and because heterogeneity in regional LV function in NIDCM patients has been noted by several studies,[15–17] we hypothesized that some NIDCM patients would show ESTE even in the non-Q-wave leads in association with severe LV wall motion abnormalities caused by non-ischemic myocardial damage.

On the basis of these considerations, we retrospectively reviewed 12-lead ECG recordings obtained during CPET in NIDCM patients with narrow QRS complexes that were suitable for ST-segment analysis. The purpose of the study was to determine whether ESTE might occur in these NIDCM patients, and, if so, to evaluate its clinical and prognostic significance.

Methods

Study Population

We studied 426 consecutive patients with NIDCM who underwent symptom-limited CPET between December 1996 and December 2005. The inclusion criteria were the presence of New York Heart Association (NYHA) class I–III, a reduction in LV ejection fraction (LVEF) below 45% evaluated by LV angiography, no previous history of coronary artery disease, and angiographic evidence of normal coronary arteries. All patients were optimally treated from a pharmacological standpoint at the time of exercise testing. The final diagnosis of NIDCM was based on the definition of the World Health Organization/International Society and Federation of Cardiology Task Force;[3] 57 patients with wide QRS complexes (≥120 ms) on resting ECG (complete left bundle-branch block in 40, complete right branch block in 6 and ventricular pacing rhythm in 11), 4 patients who developed ventricular tachyarrhythmia during or immediately after CPET, 3 patients who died of non-cardiac causes and 2 patients who could not be followed up after discharge were excluded from the present study.

CPET Procedure and Data Acquisition

Symptom-limited CPET was performed on an upright bicycle ergometer in a ramp fashion, as described previously.[18–21] We used a regularly calibrated, electronically braked cycle ergometer (Rehcor, Lode, Groningen, The Netherlands). After a resting period of at least 2 min, exercise was begun with a 1-min warm up at 0 Watt, followed by 10–20 W incremental loading every minute. Respiratory gas analysis was performed with a respiromonitor AE-280 SRC (Minato Products, Tokyo, Japan). $\dot{V}O_2$, CO_2 production, and minute ventilation data were stored in a computer hard disk every 6 s for off-line analysis. Throughout the testing, we continuously monitored 12-lead ECG (V_2, V_5, and aV_F) and heart rate, while recording hardcopies (paper speed 25 mm/s) every 1 or 2 min (Stress System ML-6500, Fukuda Denshi, Tokyo, Japan), which were used for the evaluation of ESTE. Significant ESTE was defined as ≥1.0 mm (0.1 mV) ST-segment elevation compared with the resting level measured at the J-point in at least 2 leads (except aV_R) and on at least 3 consecutive beats, at peak exercise or in the early recovery period up to 1 min. Using a cuff sphygmomanometer, arterial systolic and diastolic blood pressures were measured every minute during exercise, at peak exercise (peak systolic blood pressure, peak SBP), and every 1–2 min during recovery.

Peak $\dot{V}O_2$ was determined as the higher value of either the greatest $\dot{V}O_2$ during exercise (smoothed after a 5-point moving average) or the average $\dot{V}O_2$ in the last 3 points (18 s) before termination of exercise. The slope of linear regression relating minute ventilation to CO_2 output (ie, the $\dot{V}E/\dot{V}CO_2$ slope) between the beginning of the exercise and the respiratory compensation point was used as an index of the ventilatory response to exercise.

Follow-up Events and Prognosis

Patients were followed up for major cardiac events and hospitalization for HF after CPET from medical chart reviews and through telephone interviews. Major cardiac events were defined as a composite of cardiac death, heart transplantation or implantation of a LV assist system (LVAS).

Statistical Analysis

All data are presented as mean±standard deviation (SD). Student's t-test or Mann-Whitney U-rank test was used for comparison of continuous variables to determine the significance of differences between groups. Univariate and multivariate survival analyses were performed with the Cox proportional hazards model. For the multivariate model, we included clinical variables (age, sex and LVEF) and exercise test parameters including peak $\dot{V}O_2$, peak work rate, peak SBP, and $\dot{V}E/\dot{V}CO_2$ slope. For analysis of major cardiac events and hospitalization for HF, Kaplan-Meier estimation using a log-rank test was used. Values with $P<0.05$ were considered statistically significant. All statistical analyses were made using JMP software for Windows version 8.0.2 (SAS Inc, Cary, NC, USA).

This study was approved by the institutional review board, and was conducted in accordance with the ethical principles of the Declaration of Helsinki.

Results

Characteristics of the Patients

We enrolled 360 patients with NIDCM (289 men, 71 women) in the study. Their baseline characteristics are shown in Table 1. The mean age was 48±15 years, and 19% were in NYHA functional class I, 57% in class II and 24% in class III. LV angiography showed a mean LVEF of 26±8%. Echocardiographic examination of the LV dimensions showed a mean end-diastolic dimension of 65±9 mm and end-systolic dimension of

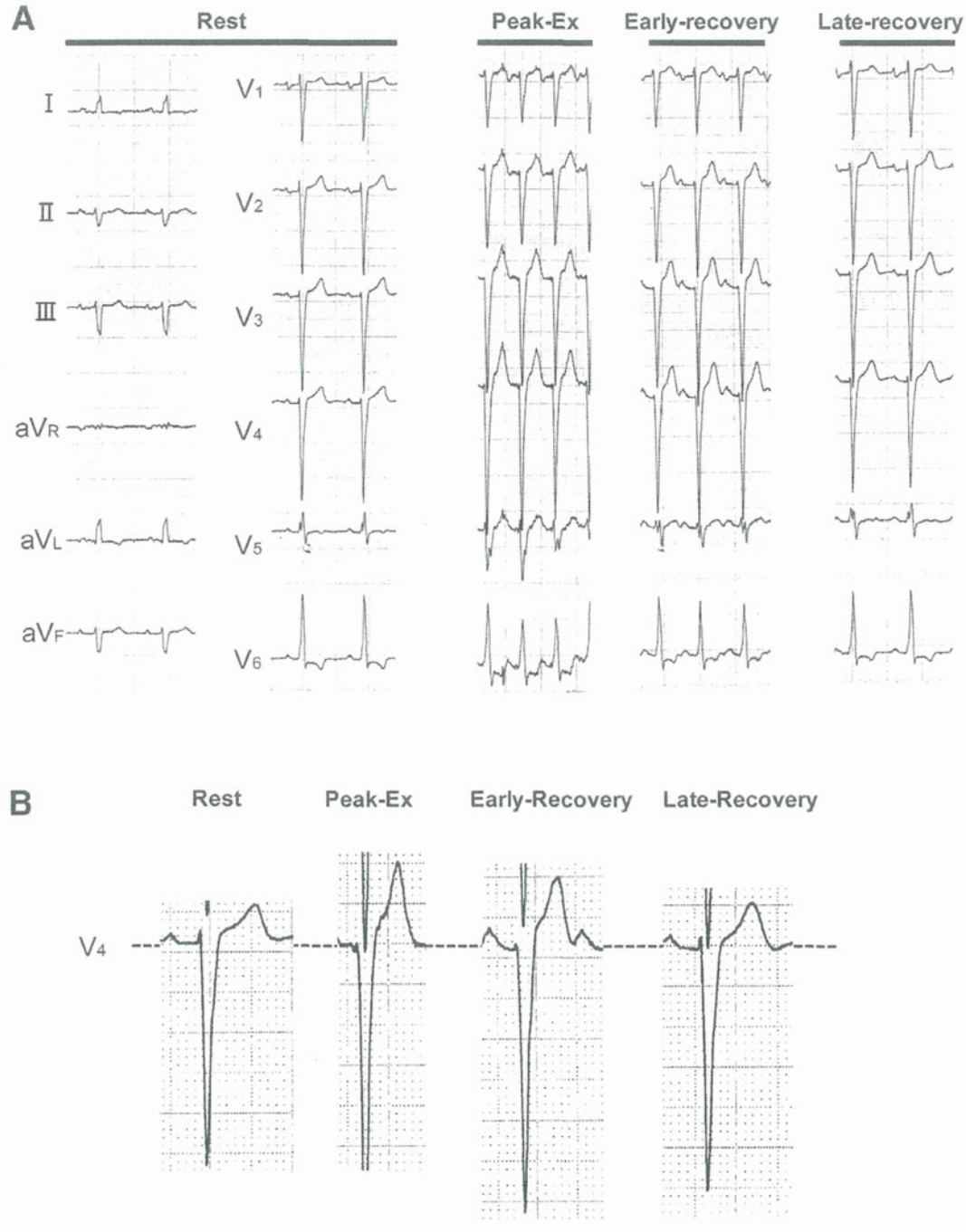

Figure 1. Representative ECG tracings showing exercise-induced ST elevation (ESTE). (**A**) 12-lead ECGs at rest and precordial lead ECGs at peak exercise (Peak-Ex), and at 2 min (Early-recovery) and 6 min (Late-recovery) after exercise. Note the ST elevation of 1.0–1.5 mm in V_3 and V_4 at peak exercise and Early-recovery, which returned to the resting level in Late-recovery. (**B**) Enlarged ECG tracings from V_4 showing maximum ESTE.

54±11 mm. As for exercise test parameters, peak work rate, peak $\dot{V}O_2$ and $\dot{V}E/\dot{V}CO_2$ slope were 116±38 W, 20.4±5.2 ml·min^{-1}·kg^{-1}, and 30±7, respectively (**Table 1**). As for medications, 234 (65%) and 316 patients (88%) were taking β-blocking agents and angiotensin-converting enzyme inhibitors or angiotensin-receptor blockers, respectively.

Clinical Profiles and Outcomes of Patients With and Without ESTE

Among the 360 patients, significant ESTE was found in 50 (13.9%), none of whom had complained of anginal symptoms during or after exercise. It was recognized in the precordial leads (V_{1-6}), except in 1 patient (aV_F). None of the 360 tested patients developed bundle-branch block (QRS width ≥120 ms)

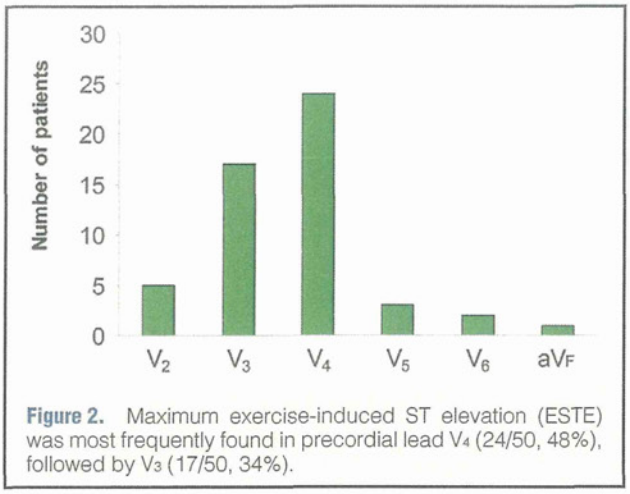

Figure 2. Maximum exercise-induced ST elevation (ESTE) was most frequently found in precordial lead V_4 (24/50, 48%), followed by V_3 (17/50, 34%).

during exercise. Representative 12-lead ECG tracings with ESTE are shown in Figure 1. The mean magnitude of the maximum ESTE in the 50 patients was 1.5±0.4 mm (range 1.0–3.0 mm). In these patients, the maximum ST elevation appeared in lead V_4 (24/50, 48%) or V_3 (17/50, 34%), as shown in Figure 2. Clinical profiles and exercise test parameters are summarized in Table 2. Between the patients with and without ESTE, age and sex did not differ significantly. LVEF was significantly and markedly lower in patients with than in those without ESTE (20±7% vs. 27±7%, P<0.001). Patients with ESTE showed significantly lower peak work rate, peak SBP, and peak $\dot{V}O_2$ than those without ESTE; however, the difference in $\dot{V}E/\dot{V}CO_2$ slope between the 2 groups was statistically marginal (P=0.04), and that in peak $\dot{V}O_2$ (P=0.01) was less pronounced compared with that in LVEF or echocardiographic dimensions (P<0.001 for all comparisons). The use of β-blocking agents was not significantly different between patients with and without ESTE (74% and 64%, respectively, P=0.15).

During the follow-up period of 52±24 months, major cardiac events (cardiac death, heart transplantation, and LVAS implantation) occurred in 106 patients and 123 patients were hospitalized for HF. In the group without ESTE, 89 patients (29%) were hospitalized for HF and major cardiac events occurred in 76 patients (25%). In contrast, among patients with ESTE, 34 patients (68%) were admitted to the hospital for HF and major cardiac events occurred in over half of the patients (30/50, 60%). Kaplan-Meier survival curves were distinctly different from each other (Figures 3A,B). Event-free survival rates for major cardiac events at 48 months in patients with and without ESTE were 61% and 88%, respectively.

Multivariate Analysis

Table 3 shows the results of Cox proportional hazard analyses. Univariate analysis revealed that NYHA, LVEF, peak SBP, peak $\dot{V}O_2$, peak work rate, $\dot{V}E/\dot{V}CO_2$ slope and ESTE were significantly related to major cardiac events. By multivariate analysis, ESTE was the only independent predictor of outcomes among the exercise test parameters.

Improved Predictability of Major Cardiac Events by the Combined Use of Peak $\dot{V}O_2$ and ESTE

Predictability of major cardiac events by using ESTE and peak $\dot{V}O_2$ is shown in Table 4. In the patient group without ESTE, major cardiac events occurred more frequently in patients with a low peak $\dot{V}O_2$ ($<14\,ml\cdot min^{-1}\cdot kg^{-1}$) than in those with a preserved peak $\dot{V}O_2$ ($\geq 14\,ml\cdot min^{-1}\cdot kg^{-1}$, 39% vs. 23%, P<0.05). In contrast, in the patient group with ESTE, the event rates were similarly high irrespective of the level of peak $\dot{V}O_2$. The presence of ESTE predicted major cardiac events with a sensitivity of 28% and a specificity of 92%, whereas low peak $\dot{V}O_2$ did with a sensitivity of 16% and specificity of 91%. In addition, because only 8 patients fulfilled both criteria (low peak $\dot{V}O_2$ and ESTE), the combined use of the criteria substantially increased the sensitivity to 39% with minimal compromise of specificity (84%).

Discussion

The major findings of this study are: (1) ESTE was found in a substantial proportion of patients with NIDCM (13.9%, n=50/360) who did not have any coronary artery lesions or

Table 2. Clinical and Exercise Test Variables of NIDCM Patients With and Without ESTE

	ESTE (–)	ESTE (+)	P value
n	310	50	
Age (years)	49±15	43±15	0.355
Sex (M/F)	251/59	38/12	0.413
BMI	22.5±3.8	21.5±3.9	0.073
NYHA	2.0±0.7	2.4±0.7	0.002
LVEF (%)	27±7	20±7	<0.001
LVDd (mm)	64±9	72±10	<0.001
LVDs (mm)	53±9	64±11	<0.001
Exercise time (s)	475±139	426±119	0.022
Peak work rate (W)	118±38	103±32	0.010
Peak SBP (mmHg)	159±36	135±34	<0.001
Peak $\dot{V}O_2$ ($ml\cdot min^{-1}\cdot kg^{-1}$)	20.7±5.2	18.6±4.7	0.009
$\dot{V}E/\dot{V}CO_2$ slope	30±7	32±8	0.035
Peak RER	1.25±0.12	1.26±0.11	0.904

Values were expressed as the mean±SD. *P<0.05 vs. group without ESTE.
BMI, body mass index; ESTE, exercise-induced ST-segment elevation; NIDCM, non-ischemic dilated cardiomyopathy. Other abbreviations as in Table 1.

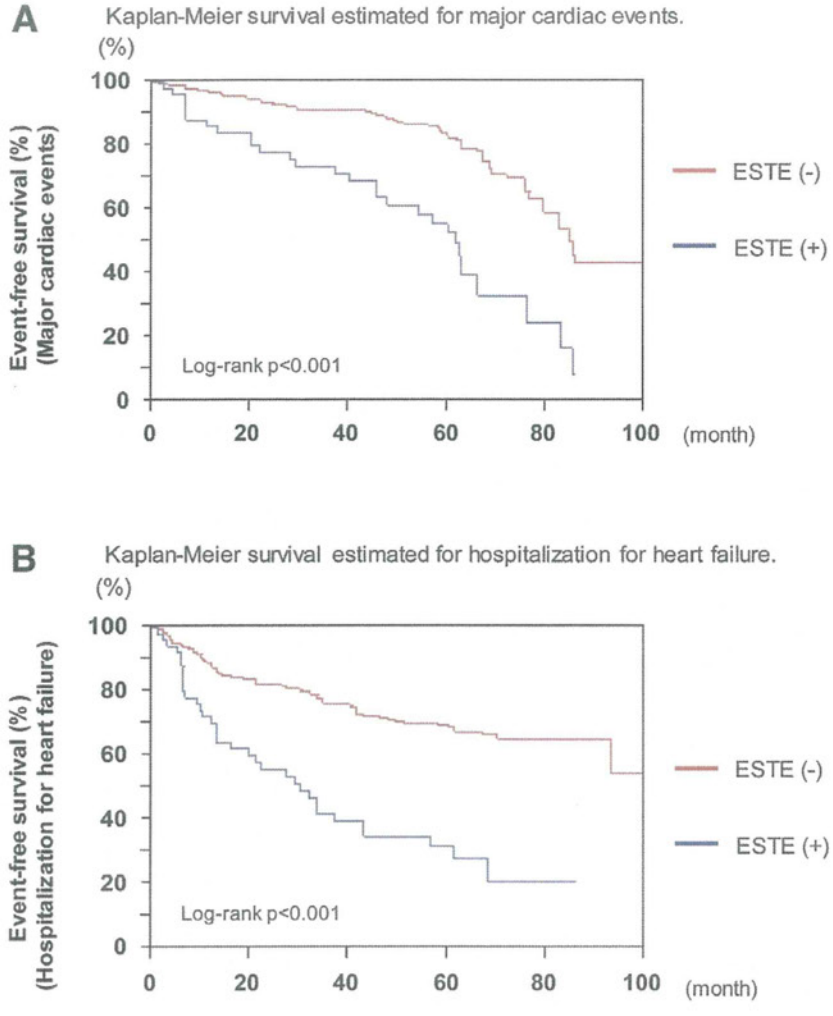

Figure 3. Kaplan-Meier event-free survival curves. (**A**) Major cardiac events (cardiac death, heart transplantation, or LVAS implantation). (**B**) Hospitalization for heart failure. The blue and red lines respectively indicate patient groups with and without exercise-induced ST elevation. LVAS, LV assist device.

Table 3. Uni/Multivariate Analyses for Cardiac Events in Patients With NIDCM

	Univariate analysis		Multivariate analysis	
	HR (95% CI)	P value	HR (95% CI)	P value
Age	0.99 (0.98–1.00)	0.052	1.01 (0.98–1.04)	0.433
Sex	0.73 (0.47–1.16)	0.173	1.20 (0.47–3.72)	0.721
NYHA	2.73 (1.73–4.46)	<0.001	2.38 (1.39–4.20)	0.002
LVEF	0.94 (0.92–0.97)	<0.001	1.00 (0.95–1.05)	0.990
Peak SBP	0.98 (0.98–0.99)	<0.001	0.99 (0.97–1.01)	0.190
Peak work rate	0.99 (0.98–0.99)	<0.001	1.01 (0.99–1.03)	0.337
Peak $\dot{V}O_2$	0.94 (0.91–0.98)	0.001	0.94 (0.82–1.08)	0.397
$\dot{V}E/\dot{V}CO_2$ slope	1.04 (1.02–1.06)	<0.001	0.99 (0.96–1.06)	0.713
ESTE	3.37 (2.15–5.06)	<0.001	2.41 (1.03–5.63)	0.042

CI, confidence interval; HR, hazard ratio. Other abbreviations as in Tables 1,2.

evidence of myocardial ischemia; (2) patients with ESTE were characterized by more depressed LVEF than those without ESTE, whereas the differences in the exercise parameters (ie, peak $\dot{V}O_2$ and $\dot{V}E/\dot{V}CO_2$ slope) between patients with and without ESTE were relatively small; (3) multivariate Cox regression analysis revealed that ESTE was the only independent predictor of major cardiac events among the exercise parameters; and (4) combining peak $\dot{V}O_2$ and ESTE substantially enhanced the predictability of major cardiac events compared with either alone. This is the first report demonstrating that NIDCM patients without any evidence of myocardial ischemia exhibit ESTE, which provides important clinical information.

Table 4. Prediction of Major Cardiac Events by ESTE and Peak $\dot{V}O_2$

	Major cardiac event rate
ESTE (–)	
Peak $\dot{V}O_2$ ≥14 ml·min^{-1}·kg^{-1}	63/277 (23%)
Peak $\dot{V}O_2$ <14 ml·min^{-1}·kg^{-1}	13/33 (39%)
ESTE (+)	
Peak $\dot{V}O_2$ ≥14 ml·min^{-1}·kg^{-1}	26/42 (62%)
Peak $\dot{V}O_2$ <14 ml·min^{-1}·kg^{-1}	4/8 (50%)

Abbreviations as in Tables 1,2.

Clinical and Prognostic Significance of ESTE in NIDCM Patients

The occurrence of ESTE was associated with more impaired functional status (NYHA and peak $\dot{V}O_2$) and more severely depressed LV function (LVEF), which provides prognostic information. During the follow-up period, major cardiac events (cardiac death, heart transplantation, or LVAS implantation) occurred in approximately half (30/50, 60%) of these patients, while only 25% of the patients without ESTE experienced cardiac events (76/310). Hospitalization for HF also occurred much more frequently in patients with ESTE (34/50, 68%) than in those without ESTE (89/310, 29%). Kaplan-Meier survival analysis revealed that the event-free survival rate for major cardiac events at 48 months was 61% and 88% in patients with and without ESTE, respectively. Multivariate Cox regression analysis showed that ESTE was independently related to outcomes after adjustment for other variables. Thus, ESTE seen in NIDCM patients has important clinical and prognostic significance.

Possible Mechanism Responsible for ESTE

The underlying mechanism(s) for the occurrence of ESTE in our NIDCM patients is unclear. Nevertheless, the hypothesis that regional LV wall motion abnormalities potentially exaggerated by exercise may contribute to the genesis of this abnormal ECG finding can be inferred from the following considerations and observations.

ESTE was most commonly observed in patients with a previous MI.[8–13] It appeared in abnormal Q-wave leads in approximately 30% of patients with anterior MI and 15% of those with inferior MI tested early after the index MI.[9,22] Although several studies suggest that ESTE represents residual demand ischemia in viable myocardium within the infarct area,[9,22] the presence of abnormal LV wall motion and/or LV aneurysm is probably the underlying mechanism in most cases. Exercise stress would exaggerate regional LV wall motion abnormalities, thereby causing new or further ST elevation similar to that observed in post-infarct patients with persistent rest ST-elevation and aneurysm.[23] On the other hand, NIDCM is generally presumed to diffusely involve the myocardium with resultant LV dilation and global hypokinesis. However, heterogeneity in regional LV function in NIDCM has long been recognized by several studies using echocardiography and other techniques, suggesting that LV wall motion is not always diffusely hypokinetic and that regional differences in the degree of hypokinesis are frequently present.[15–17] Thus, even in the absence of previous MI, some of NIDCM patients (especially those with markedly severe LV dysfunction) may have regional LV wall motion abnormalities as the possible cause of ESTE. Even though regional wall motion abnormalities would be hardly discernible at rest, exercise stress would amplify them, thereby causing ESTE. This hypothesis is still speculative, however, the results of our previous study examining patients with arrhythmogenic right ventricular cardiomyopathy without overt LV involvement and with normal coronary arteries supports it. In that study, 11 of 17 patients exhibited ESTE (≥1.0 mm) at the J-point, which appeared most frequently in the right-sided precordial leads (reflecting the area of markedly dilated right ventricle, V_{1-3} in 9 patients) and was closely associated with severe right ventricular asynergy.[14] The finding reported by Kobayashi et al[23] that ESTE was recognized in lead V_1 after right ventricular infarction, is in line with our observations.

Taken together, it is conceivable that regional wall motion abnormalities of either the left or right ventricle resulting from primary myocardial damage (ie, non-ischemic) would cause ST elevation during exercise in leads corresponding to the wall motion abnormalities. We most frequently found ESTE in leads V_4 and V_3, reflecting the anterior wall area, which is compatible with the aforementioned studies indicating that severe regional LV hypokinesis is more likely to be found in the anterior or anteroseptal wall than in the posterior or lateral area.[16,24] Future studies are necessary to confirm this hypothesis.

ESTE and Peak $\dot{V}O_2$ for Predicting Adverse Events

Recent advances in therapies for HF are remarkable,[25] but the prognosis of patients with HF, including NIDCM patients, remains poor. Identification of new measures associated with adverse events would allow better risk stratification and potentially provide opportunities for intensive treatment. In this context, the present study suggests that a simple ECG marker (ie, ESTE) can serve as a marker of poor prognosis in NIDCM patients with narrow QRS complexes on ECG. This should be of value, especially for hospitals where CPET equipment is not available.

Despite severe LV dysfunction (LVEF, 26±8%), our NIDCM patients had preserved peak $\dot{V}O_2$ (20.4±5.2 ml·min^{-1}·kg^{-1}) compared with that reported by others.[26] This is most readily explained by their non-ischemic etiology: (1) they were relatively young (48±15 years old) and (2) they were mostly thin (body mass index, 22.4±3.8), leading to overestimation of peak $\dot{V}O_2$ relative to body weight. The peak $\dot{V}O_2$ value was almost identical to that reported by Okita et al who examined Japanese HF patients with mostly non-ischemic cardiomyopathy.[25] Maximal effort evidenced by high peak RER (1.26±0.13) may also contribute to the result.

Although patients with ESTE had greater LV dysfunction ($P<0.001$) and worse prognosis than those without ESTE, the differences in peak work rate ($P=0.01$), peak $\dot{V}O_2$ ($P=0.01$), and $\dot{V}E/\dot{V}CO_2$ slope ($P=0.04$) were small. The exact reason remains unclear; however, ESTE will not appear until a significant increase in LV wall stress develops under a certain level of exercise intensity is achieved. Although ESTE was the strongest independent predictor of major cardiac events among the exercise parameters, the predictability was not high enough (sensitivity 28%, specificity 92%). Meanwhile, among the 50 patients with ESTE, a considerable number (n=26) of them with preserved peak $\dot{V}O_2$ (≥14 ml·min^{-1}·kg^{-1}) experienced major cardiac events (Table 4). This finding was advantageous for more accurately predicting cardiac events; the combination of ESTE and low peak $\dot{V}O_2$ (<14 ml·min^{-1}·kg^{-1}) substantially increased the sensitivity to 39% with minimal loss of specificity (84%). Of note, among the patients who experienced major cardiac events (n=106), only 4 exhibited both a low peak $\dot{V}O_2$ and ESTE. Furthermore, increased major cardiac event rates were associated with low peak $\dot{V}O_2$ in patient without ESTE

(39% vs. 23%, P<0.05), but not in those with ESTE (50%, vs. 62%, NS). These observations suggest the intriguing notion that the measures of peak $\dot{V}O_2$ and ESTE may reflect different aspects of the pathophysiological processes leading to cardiac death.

Study Limitations

We acknowledge several important limitations to the present study. The cohort was a selected population of patients with varying severity of HF, including many patients with mild HF symptoms, referred to a single cardiovascular center.

Because the sensitivity of the presence of ESTE was not high enough, careful interpretation and recognition of the limitation of this finding are necessary for its application in the clinical setting. One possible reason for the low sensitivity is as follows. The peak $\dot{V}O_2$ (peak $\dot{V}O_2$: 20.4±5.2 $ml \cdot min^{-1} \cdot kg^{-1}$) was relatively higher compared with earlier studies.[26] Although the overall mean LVEF was very low, our population might have included a considerable number of patients who had responded well to medical treatment. We also can not exclude the possibility that a broad range of HF severity would influence the sensitivity in the present study. Furthermore, this was a study looking purely at an exercise variable and did not include a detailed evaluation of regional LV wall motion by echocardiography or other imaging techniques, such as myocardial perfusion scintigraphy, during exercise. Future studies are necessary to elucidate the exact mechanism responsible for ESTE in NIDCM patients.

Conclusions

We, for the first time to our knowledge, demonstrated that ESTE occurs in a substantial number of NIDCM patients with narrow QRS complexes and that it represents more severe patient status and poorer prognosis. This simple ECG measure should not be overlooked and could serve as a useful parameter for assessing NIDCM patients, particularly in hospitals without the facilities for collecting and analyzing respiratory gases during exercise.

Disclosures

The present study was not supported by any grant.

References

1. Jessup M, Brozena S. Heart failure. *N Engl J* Med 2003; **348:** 2007–2018.
2. Ho KK, Pinsky JL, Kannel WB, Levy D. The epidemiology of heart failure: The Framingham Study. *J Am Coll Cardiol* 1993; **22**(Suppl): 6A–13A.
3. Richardson P, McKenna W, Bristow M, Maisch B, Mautner B, O'Connell J, et al. Report of the 1995 World Organization/International Society and Federation of Cardiology task force on the definition and classification of cardiomyopathies. *Circulation* 1996; **93:** 841–842.
4. Fukushima N, Ono M, Nakatani T, Minami M, Konaka S, Ashikari J, et al. Strategies for maximizing heart and lung transplantation opportunities in Japan. *Transplant Proc* 2009; **41:** 273–276.
5. Fukushima N, Miyamoto Y, Ohtake S, Sawa Y, Takahashi T, Nishimura M. Early result of heart transplantation in Japan: Osaka University experience. *Asian Cardiovasc Thorac Ann* 2004; **12:** 154–158.
6. Mancini DM, Eisen H, Kussmaul W, Mull R, Edmunds LH Jr, Wilson JR. Value of peak exercise oxygen consumption for optimal timing of cardiac transplantation in ambulatory patients with heart failure. *Circulation* 1991; **83:** 778–786.
7. Francis DP, Shamim W, Davies LC, Piepoli MF, Ponikowski P, Anker SD, et al. Cardiopulmonary exercise testing for prognosis in chronic heart failure: Continuous and independent prognostic value from VE/VCO_2 slope and peak VO_2. *Eur Heart J* 2000; **21:** 154–161.
8. Bruce RA, Fisher LD, Pettigner M, Weiner DA, Chaitman BR. ST segment elevation with exercise: A marker for poor ventricular function and poor prognosis. *Circulation* 1988; **77:** 897–905.
9. Stiles GL, Rosati RA, Wallace AG. Clinical relevance of exercise induced ST segment elevation. *Am J Cardiol* 1980; **46:** 931–936.
10. Ogawa T, Ishii M, Iida K, Iida K, Ajisaka R, Yamaguchi I, et al. Mechanisms of stress-induced ST elevation and negative T-wave normalization studied by serial cardiokymogram in patients with previous myocardial infarction. *Am J Cardiol* 1990; **65:** 962–966.
11. Haines DE, Beller GA, Watson DD, Kaiser DL, Sayre SL, Gibson RS. Exercise induced ST segment elevation 2 weeks after uncomplicated myocardial infarction: Contributing factors and prognostic significance. *J Am Coll Cardiol* 1987; **9:** 996–1003.
12. Manrique A, Koning R, Hitzel A, Cribier A, Véra P. Exercise-induced ST-elevation is related to left ventricular dysfunction but not to myocardial viability in patients with healed myocardial infarction. *Eur J Heart Fail* 2001; **3:** 709–716.
13. Margonato A, Chierchia SL, Xuereb RG, Xuereb M, Fragasso G, Cappelletti A, et al. Specificity and sensitivity of exercise-induced ST segment elevation for detection of residual viability: Comparison with fluorodeoxyglucose and positron emission tomography. *J Am Coll Cardiol* 1995; **25:** 1032–1038.
14. Toyofuku M, Takaki H, Sunagawa K, Kurita T, Shimizu W, Suyama K, et al. Exercise-induced ST elevation in patients with arrhythmogenic right ventricular dysplasia. *J Electrocardiol* 1999; **32:** 1–5.
15. Yamaguchi S, Tsuiki K, Hayasaka M, Yaui S. Segmental wall motion abnormalities in dilated cardiomyopathy: Hemodynamic characteristics and comparison with thallium-201 myocardial scintigraphy. *Am Heart J* 1987; **113:** 1123–1128.
16. Sunnerhagen KS, Bhargava V, Shabetai R. Regional left ventricular wall motion abnormalities in idiopathic dilated cardiomyopathy. *Am J Cardiol* 1990; **65:** 364–370.
17. Young AA, Dakos S, Powell KA, Sturm B, McCulloch AD, Starling RC. Regional heterogeneity of function in nonischemic dilated cardiomyopathy. *Cardiovasc Res* 2001; **49:** 308–318.
18. Takaki H, Sakuragi S, Nagaya N, Suzuki S, Goto Y, Sato T, et al. Postexercise VO_2 "hump" phenomenon as an indicator for inducible myocardial ischemia in patients with acute anterior myocardial infarction. *Int J Cardiol* 2006; **111:** 67–74.
19. Tomita T, Takaki H, Hara Y, Sakamaki F, Satoh T, Takagi S, et al. Attenuation of hypercapnic carbon dioxide chemosensitivity after postinfarction exercise training: Possible contribution to the improvement in exercise hyperventilation. *Heart* 2003; **89:** 404–410.
20. Nishi I, Noguchi T, Iwanaga Y, Furuichi S, Aihara N, Takaki H, et al. Effects of exercise training in patients with chronic heart failure and advanced left ventricular systolic dysfunction receiving β-blockers. *Circ J* 2011; **75:** 1649–1655.
21. Kamakura T, Kawakami R, Nakanishi M, Ibuki M, Ohara T, Yanase M, et al. Efficacy of out-patient cardiac rehabilitation in low prognostic risk patients after acute myocardial infarction in primary intervention era. *Circ J* 2011; **75:** 315–321.
22. de Feyter PJ, Majid PA, van Eenige MJ, Wardeh R, Wempe FN, Roos JP. Clinical significance of exercise-induced ST segment elevation: Correlative angiographic study in patients with ischemic heart disease. *Br Heart J* 1981; **46:** 84–92.
23. Kobayashi H, Tsuchihashi K, Hashimoto A, Nagao K, Tanaka S, Shimamoto K, et al. Exercise-induced STV_1 elevation: A sign of right ventricular dysfunction in recent inferior myocardial infarction. *Can J Cardiol* 1994; **10:** 355–362.
24. Bach DS, Beanlands RS, Schwaiger M, Armstrong WF. Heterogeneity of ventricular function and myocardial oxidative metabolism in nonischemic dilated cardiomyopathy. *J Am Coll Cardiol* 1995; **25:** 1258–1262.
25. Okita K, Yonezawa K, Nishijima H, Hanada A, Ohtsubo M, Kohya T, et al. Skeletal muscle metabolism limits exercise capacity in patients with chronic heart failure. *Circulation* 1998; **98:** 1886–1891.
26. Poggio R, Arazi HC, Giorgi M, Miriuka SG. Prediction of severe cardiovascular events by VE/VCO_2 slope versus peak VO_2 in systolic heart failure: A meta-analysis of the published literature. *Am Heart J* 2010; **160:** 1004–1014.

Acta Physiol 2013, 207, 494–502

High-frequency dominant depression of peripheral vagal control of heart rate in rats with chronic heart failure

T. Kawada,[1] M. Li,[1] S. Shimizu,[1] A. Kamiya,[1] K. Uemura,[1] M. J. Turner,[1] M. Mizuno[2] and M. Sugimachi[1]

1 Department of Cardiovascular Dynamics, National Cerebral and Cardiovascular Center, Osaka, Japan

2 Department of Health Care Sciences, University of Texas Southwestern Medical Center, Dallas, TX, USA

Received 2 November 2012,
revision requested 2 December 2012,
revision received 5 December 2012,
accepted 15 December 2012
Correspondence: T. Kawada, MD, PhD, Department of Cardiovascular Dynamics, National Cerebral and Cardiovascular Center Research Institute, 5-7-1 Fujishiro-dai, Suita, Osaka 565-8565, Japan.
E-mail: torukawa@ri.ncvc.go.jp

Abstract

Aim: To examine whether dynamic characteristics of the peripheral vagal control of heart rate (HR) are altered in chronic heart failure (CHF).

Methods: The right vagal nerve was electrically stimulated according to a binary white noise signal, and the transfer function from vagal nerve stimulation (VNS) to HR was estimated in the frequency range from 0.01 to 1 Hz in five control rats and five CHF rats under anaesthetized conditions. The rate of VNS was changed among 10, 20 and 40 Hz.

Results: A multiple linear regression analysis indicated that the increase in the VNS rate augmented the ratio of the high-frequency (HF) gain to the steady-state gain in the control group but not in the CHF group. As a result, the dynamic gain of the transfer function in the frequencies near 1 Hz decreased more in the CHF group than in the control group.

Conclusion: Changes in the dynamic characteristics of the peripheral vagal control of HR may contribute to the manifestation of decreased HF components of HR variability observed in CHF.

Keywords transfer function, vagal nerve stimulation, white noise analysis.

Heart rate (HR) is mainly governed by the autonomic nervous system. The dynamic HR response to autonomic nervous activity is important for moment-to-moment adjustments of cardiac function during daily activity. High-frequency (HF) components of HR variability (HRV) are considered to be an index of vagal nerve activity, because the dynamic HR response to vagal nerve activity is faster than that to sympathetic nerve activity (Akselrod *et al.* 1981, Berger *et al.* 1989, Kawada *et al.* 1996, Mizuno *et al.* 2010). The HF components of HRV are known to be decreased in diseased conditions such as chronic heart failure (CHF; Task Force of the European Society of Cardiology 1996, Olshansky *et al.* 2008). The interpretation of the HF components can depend on the input–output transduction property from vagal nerve activity to HR. For instance, the decreased HF components may indicate diminished vagal outflow from the central nervous system if the transduction property is not changed between normal and CHF conditions. On the other hand, there is also a possibility that the decreased HF components are merely the result of impaired transduction property from vagal nerve activity to HR in the HF range. To better understand the significance of the decreased HF components of HRV observed in CHF, quantification of the transduction property becomes essential.

The input–output transduction property of a biological system usually reveals dynamic characteristics (Sagawa 1983). That is to say, the amplitude and the phase lag of the system response vary depending on the frequency of the input modulation. In the case of the vagal control of HR, the transduction property has low-pass characteristics (Berger *et al.* 1989, Kawada *et al.* 1996, Mizuno *et al.* 2010). The amplitude of the HR response is large when the frequency of vagal modulation is low, and the amplitude of the HR response becomes smaller as the frequency of vagal

modulation increases. It remains unknown, however, whether the dynamic characteristics of the peripheral vagal control of HR are altered in CHF. To test the hypothesis that dynamic characteristics of the peripheral vagal control of HR are altered in CHF, the transfer functions from efferent vagal nerve stimulation (VNS) to HR were compared between normal control rats and rats with CHF following myocardial infarction.

Materials and methods

The study is conform with Good Publishing Practice in Physiology (Persson & Henriksson 2011). Experiments were performed on adult male Sprague–Dawley rats.

CHF rats

Myocardial infarction was induced under halothane anaesthesia by ligating the left coronary artery in 8-week-old rats according to a previously established procedure (Li *et al.* 2004, Kawada *et al.* 2010). After recovered from the anaesthesia, the rats were fed with standard laboratory chow *ad libitum* and with free access to water. Rats that survived for 8 weeks after myocardial infarction were used for the CHF group.

Animal preparation

Rats were anaesthetized with an intraperitoneal injection (2 mL kg^{-1}) of a mixture of urethane (250 mg mL^{-1}) and α-chloralose (40 mg mL^{-1}), followed by a maintenance dose of intravenous continuous infusion of the anaesthetic mixture. The trachea was intubated and artificial ventilation was performed. An arterial catheter was inserted into the right femoral artery to monitor arterial pressure. A body surface electrocardiogram was recorded, and HR was detected through use of a cardiotachometer.

To avoid a possible contribution from reflexes arising from cardiopulmonary regions and aortic arch, the vagi and the aortic depressor nerves were sectioned at the neck. To minimize reflex changes in efferent sympathetic nerve activity, bilateral carotid sinuses were isolated from the systemic circulation (Shoukas *et al.* 1991, Sato *et al.* 1999, Kawada *et al.* 2010), and intracarotid sinus pressure was held at 120 mmHg during VNS.

A pair of stainless steel wire electrodes (Bioflex wire, AS633; Cooner Wire, Chatsworth, CA, USA) was attached to the sectioned distal end of the right cervical vagus for efferent VNS. The nerve and electrodes were secured and insulated with silicone glue (Kwik-Sil; World Precision Instruments, Sarasota, FL, USA). The pulse duration was set to 2 ms. The pulse amplitude was set to supramaximal in each rat using 10-Hz constant VNS so that increasing the amplitude did not further decrease HR. The resultant amplitude ranged from 2.0 to 3.5 V.

Protocols

In five control rats and five CHF rats, VNS was turned on and off every 500 ms according to a binary white noise signal. The input power spectrum of VNS was reasonably constant up to 1 Hz, and the transfer function from VNS to HR was estimated up to 1 Hz. Three intensities of VNS (10, 20 and 40 Hz) were tested in random order in each rat. To avoid possible confusion in later transfer function descriptions, VNS frequency will hereafter be referred to as the VNS rate. The binary white noise input using each VNS rate was applied for 15 min.

Data analysis

Data were sampled at 1000 Hz using a 16-bit analogue-to-digital converter and stored on a dedicated laboratory computer system. The transfer function from VNS to HR was estimated by treating VNS as the system input perturbation and HR as the system output response (Mizuno *et al.* 2010). The coherence was also calculated as an index of linear dependence of the system output on the input perturbation. The coherence takes values from zero to unity. Zero coherence indicates total independence between the input and output signals. Unity coherence indicates that the output was perfectly explained by linear dynamics of the input.

Transfer function model

While we previously used a first-order low-pass filter with pure dead time to describe the transfer function from VNS to HR in rabbits (Kawada *et al.* 1996, Nakahara *et al.* 1998, Miyamoto *et al.* 2004, Mizuno *et al.* 2007), this model was not necessarily the best model to describe the transfer function from VNS to HR in rats (Mizuno *et al.* 2010). To better describe the estimated transfer function in rats, we employed a following new model (Kawada *et al.* 2012):

$$H(f) = -K\left(\frac{1-R}{1+\frac{f}{f_C}j}+R\right)e^{-2\pi fLj}$$

where j denotes the imaginary units; K (in bpm Hz^{-1}) is the steady-state gain which is an asymptote of dynamic gain of $H(f)$ as the frequency tends to zero; f_C (in Hz) is the corner frequency corresponding to a first-order low-pass filter; L (in s) is the pure dead

time; and R (no units) is the ratio of the HF gain to the steady-state gain. As the frequency increases beyond the corner frequency toward infinity, the dynamic gain of $H(f)$ asymptotically approaches KR. When R equals zero, $H(f)$ reduces to a simple first-order low-pass filter with pure dead time used in the previous studies. Hereafter in this study, R is referred to as 'relative HF gain'.

Statistical analysis

All data are presented as mean ± SE. Differences in transfer function parameters were analysed by a multiple linear regression as follows (Glantz & Slinker 2001):

$$p = C + B_{VNS} \times D_{VNS} + B_{CHF} \times D_{CHF} + B_{Interaction} \times D_{VNS} \times D_{CHF} + B_{m1} \times D_{m1} + \cdots + B_{m4} \times D_{m4} + B_{n1} \times D_{n1} + \cdots + B_{n4} \times D_{n4}$$

where p represents each parameter value; C is a constant term or an intercept of the multiple linear regression; B_{VNS} is a coefficient for the VNS effect; D_{VNS} is a dummy variable encoding the VNS rate ($D_{VNS} = 0$ for 10 Hz, $D_{VNS} = 1$ for 20 Hz, and $D_{VNS} = 2$ for 40 Hz); B_{CHF} is a coefficient for the CHF effect; D_{CHF} is a dummy variable encoding the CHF animals ($D_{CHF} = 0$ for the control rats, and $D_{CHF} = 1$ for the CHF rats); $B_{Interaction}$ is a coefficient for the interaction effect between D_{VNS} and D_{CHF}; D_{m1} through D_{m4} are dummy variables encoding five different animals in the control group; D_{n1} through D_{n4} are dummy variables encoding five different animals in the CHF group (see Table 1); and B_{m1} through B_{m4} and B_{n1} through B_{n4} are coefficients for inter-individual variations. Note that C is an estimate of the parameter value corresponding to the transfer function obtained by 10-Hz VNS ($D_{VNS} = 0$) in the control group ($D_{CHF} = 0$). B_{VNS}, B_{CHF}, and $B_{Interaction}$ were tested as to whether they were significantly different from zero, with a significance level set at $P < 0.05$ (Glantz & Slinker 2001).

Table 1 Dummy variables encoding experimental animals

	D_{m1}	D_{m2}	D_{m3}	D_{m4}	D_{n1}	D_{n2}	D_{n3}	D_{n4}
Control no. 1	1	0	0	0	0	0	0	0
Control no. 2	0	1	0	0	0	0	0	0
Control no. 3	0	0	1	0	0	0	0	0
Control no. 4	0	0	0	1	0	0	0	0
Control no. 5	−1	−1	−1	−1	0	0	0	0
CHF no. 1	0	0	0	0	1	0	0	0
CHF no. 2	0	0	0	0	0	1	0	0
CHF no. 3	0	0	0	0	0	0	1	0
CHF no. 4	0	0	0	0	0	0	0	1
CHF no. 5	0	0	0	0	−1	−1	−1	−1

To encode five different animals, four dummy variables are needed in each group. The encoding does not cross the boundary between the control and chronic heart failure (CHF) groups. Effects coding was used to model the inter-individual differences (Glantz & Slinker 2001).

Results

Figure 1 represents typical results obtained from a control rat. Dynamic HR responses to the binary white noise inputs using 10, 20 and 40-Hz VNS are shown in Figure 1a. After the onset of VNS, HR decreased intermittently in response to the binary VNS. As the VNS rate increased, the magnitude of dynamic HR response increased. The group-averaged decreases in mean HR relative to the pre-stimulation HR were 54 ± 4, 84 ± 14 and 137 ± 17 bpm (13 ± 1, 19 ± 3, and 32 ± 3%) during 10, 20 and 40-Hz VNS respectively. Transfer functions from VNS to HR are depicted in Figure 1b. The solid lines are the calculated transfer functions, and the grey smooth lines are the corresponding model transfer functions. The dynamic gain became smaller as the frequency increased during 10-Hz VNS, indicating low-pass characteristics of the system. The dynamic gain, however, did not fall off smoothly during 20-Hz VNS, and the gain plot exhibited a plateau in the frequencies above 0.3 Hz. The gain plot became much flatter during 40-Hz VNS. The phase approached $-\pi$ radians at the lowest frequency, reflecting the negative HR response to VNS. The coherence was close to unity in the frequencies below 0.1 Hz and decreased slightly in the frequencies above 0.1 Hz.

Figure 2 shows typical results obtained from a CHF rat. The magnitudes of dynamic HR responses to binary VNS were smaller than those in the control rat (Figs 2a vs. 1a). The rapid restorations of HR to baseline HR were not observed during 20- and 40-Hz VNS in the CHF rat. The group-averaged decreases in mean HR relative to the pre-stimulation HR were 46 ± 8, 71 ± 12 and 157 ± 24 bpm (12 ± 2, 18 ± 3 and 38 ± 6%) during 10, 20 and 40-Hz VNS respectively. The transfer function from VNS to HR

Acta Physiologica © 2012 Scandinavian Physiological Society, doi: 10.1111/apha.12055

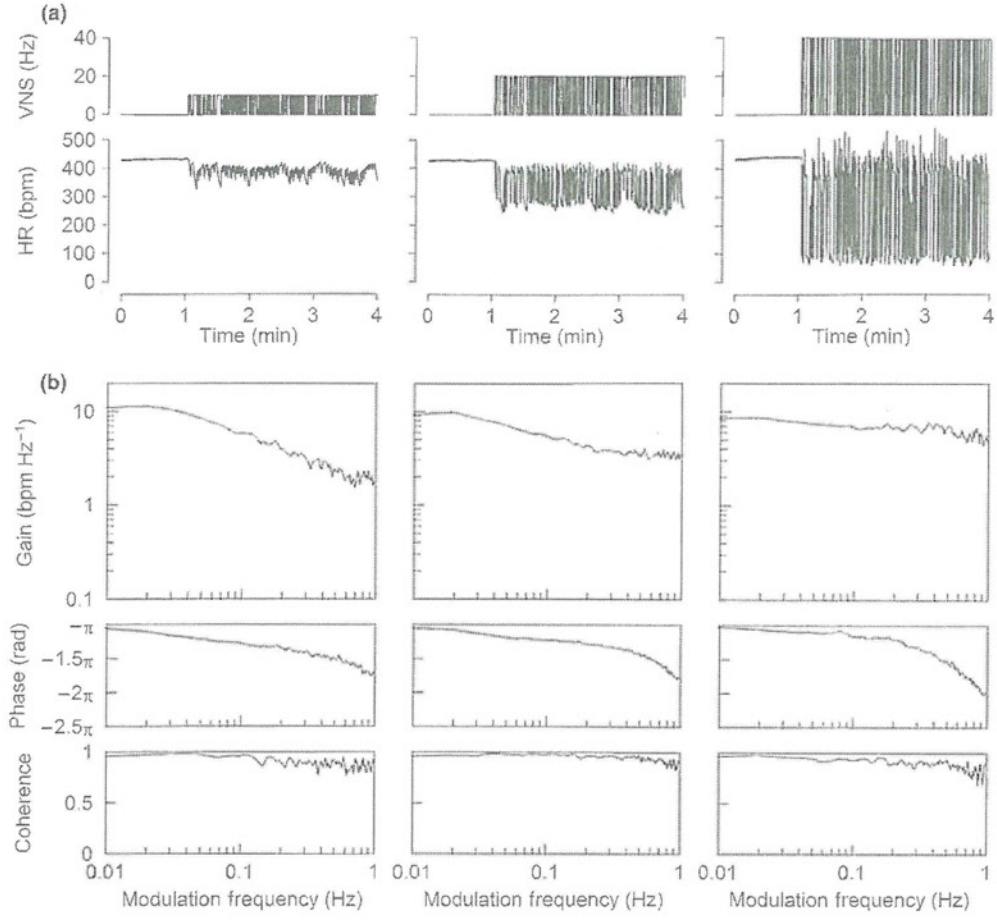

Figure 1 (a) Typical experimental data showing the binary white noise input using vagal nerve stimulation (VNS) and corresponding heart rate (HR) response in a control rat. The VNS rate was changed among 10, 20 and 40 Hz. (b) Transfer functions from VNS to HR corresponding to the time series data. The thin black lines indicate the estimated transfer functions. The bold grey lines indicate the fitting results of the model transfer functions.

revealed low-pass characteristics in the CHF rat (Fig. 2b). In contrast to the normal rat, the increase in the VNS rate did not manifest a plateau of the dynamic gain in the higher frequency range. The phase approached $-\pi$ radians at the lowest frequency and delayed smoothly as the frequency increased. The coherence was close to unity during 10-Hz VNS. There were decreases in coherence in the frequencies above 0.4 Hz during 20-Hz VNS. The coherence became lower during 40-Hz VNS compared to that during 20-Hz VNS.

Figure 3 depicts group-averaged transfer functions. The shape of the transfer function during 10-Hz VNS was similar between the control and CHF groups, except for a nearly parallel downward shift in the gain plot in the CHF group. The shape of the transfer function during 20-Hz VNS differed between the control and CHF groups in that there was a plateau in the gain plot above 0.5 Hz in the control group. The plateau in the gain plot became more overt and occurred above 0.3 Hz during 40-Hz VNS in the control group. The relative HF gain in the model transfer function is frequency independent, which means that the increase in the relative HF gain reduces the phase delay (Fig. 4b, middle). As can be seen in Figure 3, the magnitudes of phase delay from $-\pi$ radians in the higher frequency range were smaller in the control group compared to the CHF group during 20 and 40-Hz VNS. The results of the multiple linear regression analysis on the transfer function parameters are summarized in Table 2.

Discussion

Although HF components of HRV are known to be decreased in CHF (Task Force of the European Society of Cardiology 1996, Olshansky *et al.* 2008), the present study is the first to demonstrate changes in the dynamic characteristics of the peripheral vagal control of HR in CHF.

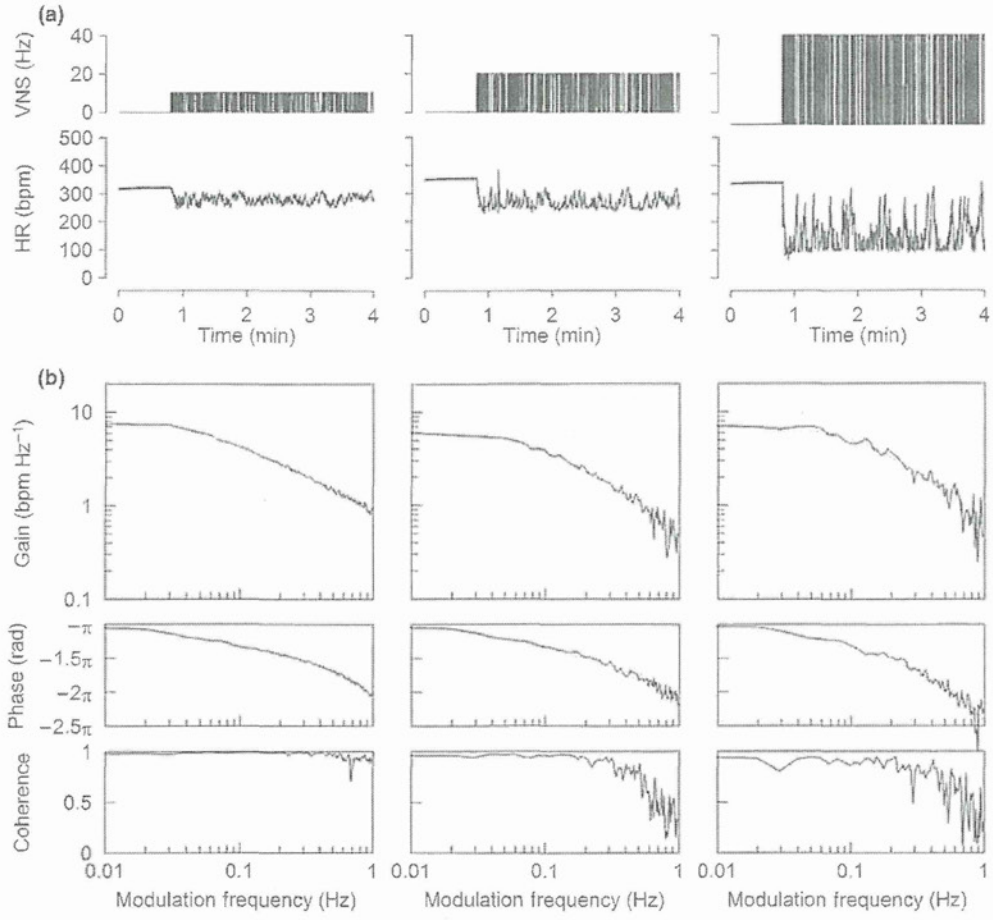

Figure 2 (a) Typical experimental data showing the binary white noise input using vagal nerve stimulation (VNS) and corresponding heart rate (HR) response in a rat with chronic heart failure. The VNS rate was changed among 10, 20 and 40 Hz. (b) Transfer functions from VNS to HR corresponding to the time series data. The thin black lines indicate the estimated transfer functions. The bold grey lines indicate the fitting results of the model transfer functions.

Effects of CHF and VNS rate on the steady-state gain

The steady-state gain, K, determines vertical location of the transduction property in the gain plot (Fig. 4a, top) without influencing the phase plot (Fig. 4a, middle). An increase in the steady-state gain is associated with an augmented step response of HR (Fig. 4a, bottom). The effect of CHF (B_{CHF}) on the steady-state gain was significantly negative (Table 2), suggesting overall depression of the peripheral vagal control of HR in the CHF group compared to the control group. Several factors are considered to attenuate the HR response to VNS as follows. Bibevski & Dunlap (1999) have suggested that parasympathetic ganglionic transmission is attenuated in heart failure. Angiotensin II, which is known to be increased in CHF conditions (Riegger 1985), attenuates myocardial interstitial acetylcholine release in response to VNS (Kawada *et al.* 2007) and reduces the dynamic gain of the transfer function from VNS to HR (Kawada *et al.* 2009). Du *et al.* (1998) demonstrated that blockade of angiotensin II type 1 receptors by losartan-enhanced bradycardia induced by VNS in rats with chronic myocardial infarction. Besides the effect of CHF, the effect of VNS rate (B_{VNS}) on the steady-state gain was also significantly negative, suggesting that the HR response became saturated and did not increase in proportion to the increased VNS rate. The decrease in the steady-state gain at higher VNS rates is consistent with the study by Berger *et al.* (1989) where the canine atrial response was examined.

Interactions exist between the sympathetic and parasympathetic nervous systems in regulating HR. In a presynaptic mechanism, noradrenaline released from the sympathetic nerve endings inhibits acetylcholine release from the vagal nerve endings through α_1-adrenergic receptors (Wetzel *et al.* 1985). In a postsynaptic mechanism, accumulation of cyclic AMP in the sinus nodal cells by β-adrenergic stimulation augments the dynamic vagal control of HR (Nakahara *et al.* 1998). Levy

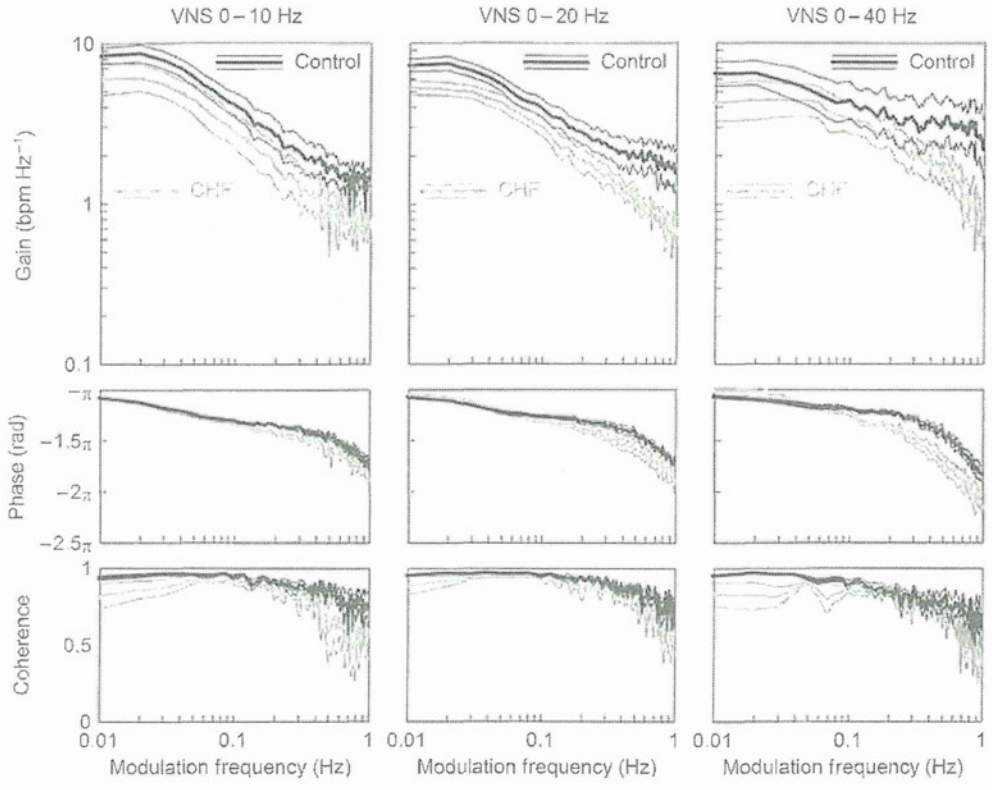

Figure 3 Group-averaged transfer functions from vagal nerve stimulation (VNS) to heart rate obtained from the control group (black lines) and the chronic heart failure (CHF) group (grey lines). The thick and thin lines indicate mean and mean ± SE respectively.

(1971) termed the phenomenon that the vagal control of HR is augmented by concomitant sympathetic activation as accentuated antagonism. In a present study, changes in efferent sympathetic nerve activity were minimized within individual animals by disabling the baroreflexes. However, it is plausible that the CHF group had higher basal sympathetic tone than the control group (Riegger 1985). While the accentuated antagonism does not conform to the attenuation of the steady-state gain, the presynaptic inhibition might have contributed to the attenuation of the steady-state gain in the CHF group.

Effects of CHF and VNS rate on the relative HF gain

The relative HF gain, R, modifies the transduction property of dynamic gain in the higher frequencies (Fig. 4b, top). An increase in the relative HF gain reduces the phase delay (Fig. 4b, middle) and enhances the initial drop seen in the step response of HR (Fig. 4b, bottom). A new finding of the present study is the augmentation in the relative HF gain with increasing the VNS rate, as evidenced by the positive B_{VNS} on the relative HF gain (Table 2). Furthermore, the effect of VNS rate on the relative HF gain was totally cancelled by the interaction effect (the negative $B_{Interaction}$ with approximately the same absolute value as the positive B_{VNS}), indicating that the increase in the VNS rate did not augment the relative HF gain in the CHF group. It can be interpreted that increasing the VNS rate enhanced the initial drop of the step response of HR in the control rats but not in the CHF rats. A previous study in rabbits has shown that a direct action of acetylcholine through muscarinic potassium (K_{ACh}) channels plays an essential role in the HR control at high VNS rates compared to a cyclic-AMP-mediated indirect pathway (Mizuno *et al.* 2007). Because K_{ACh} channels regulate rapid HR response, it is conceivable that the increase in the VNS rate increased the contribution of K_{ACh} channels, resulting in the augmentation of dynamic gain in the higher frequency range in the control group. The density of K_{ACh} channels and the sensitivity of K_{ACh} channels to G_i-mediated channel activation are reduced in atrial myocytes isolated from failing human hearts compared to donor atria (Koumi *et al.* 1994). The reduced K_{ACh} channel density and sensitivity may lead to the loss of the high VNS rate-induced augmentation in the relative HF gain in the CHF group.

Cerutti *et al.* (1991) defined the HF band in rats to be above 0.75 Hz based on the spectral analysis of

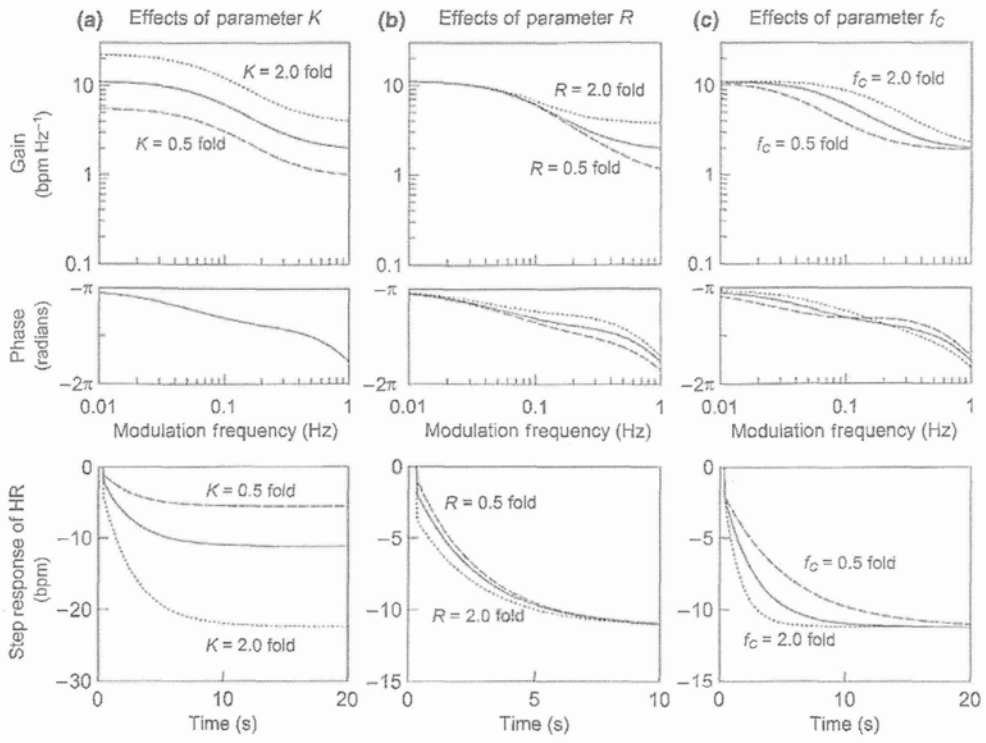

Figure 4 Schematic presentation of the effects of transfer function parameters. Gain plots (top panels), phase plots (middle panels) and step responses of heart rate (HR) derived from the transfer function (bottom panels) are shown. (a) The steady-state gain, *K*, determines overall responsiveness of HR. (b) The relative high-frequency gain, *R*, determines the magnitude of initial drop of the HR response. (c) The corner frequency, f_C, determines the rapidness of the HR response. In all panels, the solid lines represent the transfer function and step response derived from 10-Hz vagal nerve stimulation in the control group. The dotted lines indicate the effects of twofold increase in each parameter. The dashed lines indicate the effects of decreasing each parameter to 0.5-fold of the control value.

Table 2 Results of multiple linear regression analysis

	C	B_{VNS}	B_{CHF}	$B_{Interaction}$	R^2
K (bpm Hz^{-1})	8.87 ± 0.42	−0.93 ± 0.32**	−2.31 ± 0.59**	0.04 ± 0.46	0.87
f_C (Hz)	0.050 ± 0.015	0.004 ± 0.012	−0.005 ± 0.022	0.044 ± 0.017*	0.72
L (s)	0.31 ± 0.02	0.04 ± 0.02	0.03 ± 0.03	−0.0002 ± 0.027	0.54
R	0.14 ± 0.04	0.15 ± 0.03**	−0.03 ± 0.06	−0.14 ± 0.04**	0.77
−3 dB point (Hz)	0.042 ± 0.032	0.053 ± 0.025*	0.006 ± 0.046	−0.009 ± 0.035	0.49

K: steady-state gain; f_C: corner frequency; *L*: pure dead time; *R*: the ratio of high-frequency gain to the steady-state gain in the transfer function from vagal nerve stimulation (VNS) to heart rate; −3 dB point: the point at which frequency the dynamic gain decreases by 3 dB relative to the steady-state gain; C: constant; B_{VNS}: coefficient for the effect of VNS rate; B_{CHF}: coefficient for the effect of chronic heart failure (CHF); $B_{Interaction}$: coefficient for the interaction between the effects of VNS rate and CHF. *$P < 0.05$ and **$P < 0.01$ by a multiple linear regression analysis.

HRV. In this frequency band, the discrepancy in the dynamic gain between the control and CHF group became magnified during 20- and 40-Hz VNS (Fig. 3). Therefore, the depression of the HF components in CHF can occur due to changes in the dynamic characteristics of the peripheral vagal control of HR even if the vagal outflow from the central nervous system remains unchanged. The upper frequency bound of the HF band was 3.85 Hz (a half of 1/130 ms) in the study by Cerutti *et al.* (1991). In the present study, however, the transfer function was identified only up to 1 Hz. This is because HR decreased as low as 100 bpm (1.66 Hz) during intense VNS (Fig. 1a). If we assume that 1.66 Hz is an effective sampling frequency of the HR signal, the valid upper bound for the spectral calculation becomes 0.83 Hz.

Effects of CHF and VNS rate on the corner frequency

The corner frequency, f_C, determines horizontal location of the transduction property in the gain plot (Fig. 4c, top). The effect of the corner frequency on the phase plot is rather complex due to the presence of relative HF gain (Fig. 4c, middle). An increase in the corner frequency accelerates the step response of HR (Fig. 4c, bottom). The effect on the corner frequency was significantly positive only in the interaction effect ($B_{Interaction}$), suggesting that the increase in the VNS rate increased the corner frequency in the CHF group alone. However, if we calculate the corner frequency based on another definition (the point at which the dynamic gain decreases by 3 dB from the steady-state gain), the effect of VNS rate (B_{VNS}) was significantly positive and the interaction effect became insignificant (Table 2). Berger *et al.* (1989) pointed out that the dynamic gain of the transfer function fell off at a lower frequency when lower mean VNS rates were used, which is consistent with the positive effect of the VNS rate on the −3 dB point. Further studies are required to identify the mechanism for changes in the corner frequency induced by the increase in the VNS rate. Nonlinearity of the HR response may be involved in the changes in the corner frequency, because the coherence values were lower during 40-Hz VNS, especially in the CHF group.

Limitations

Several limitations need to be noticed. Because this study was performed under urethane and α-chloralose anaesthesia and surgical preparation, autonomic tone might have been different from conscious physiological conditions. The anaesthesia and surgical preparation might have also affected the autonomic control of HR. However, because we stimulated the distal end of the sectioned vagal nerve and observed the HR response under the same experimental settings, comparison between the control and CHF groups may be valid.

We have examined three intensities of VNS rate. Although comparing the VNS rate to physiologic levels is difficult, if we assume that physiologic levels of efferent vagal nerve traffic exert a 10% reduction relative to a baseline HR (Mizuno *et al.* 2011), judging from the per cent decrease in mean HR during VNS, 10-Hz VNS may be most relevant in the physiologic sense. The 40-Hz VNS must be interpreted as an extreme case.

Conclusion

We have shown that the dynamic characteristics of the peripheral vagal control of HR differ between the control and CHF groups. In the CHF group, the high VNS rate-induced augmentation in the relative HF gain was not observed. As a result, the dynamic HR response to VNS was significantly depressed in the HF range in the CHF group compared to the control group. In addition to the reduced vagal outflow from the central nervous system and attenuated parasympathetic ganglionic transmission, changes in the dynamic characteristics of the peripheral vagal control of HR may contribute to the manifestation of decreased HF components of HRV observed in CHF. The depression of the HF components does not necessarily indicate the reduced vagal outflow from the central nervous system. The VNS is explored as a replacement treatment of diminished vagal tone in CHF (Li *et al.* 2004, Schwartz 2011). Careful interpretation may be required as to the depression of HF components in CHF if it is used to assess the vagal tone for the selection of possible target patients of the VNS therapy.

Conflict of interest

The authors declare that they have no conflict of interest.

This study was supported by Health and Labour Sciences Research Grants (H19-nano-Ippan-009, H20-katsudo-Shitei-007 and H21-nano-Ippan -005) from the Ministry of Health, Labour and Welfare of Japan; and by the Grant-in-Aid for Scientific Research (C-23592319, 23-01705) promoted by the Ministry of Education, Culture, Sports, Science and Technology of Japan; and by the Industrial Technology Research Grant Program from the New Energy and Industrial Technology Development Organization (NEDO) of Japan.

References

Akselrod, S., Gordon, D., Ubel, F.A., Shannon, D.C., Berger, A.C. & Cohen, R.J. (1981) Power spectrum analysis of heart rate fluctuation: a quantitative probe of beat-to-beat cardiovascular control. *Science* 213, 220–222.

Berger, R.D., Saul, J.P. & Cohen, R.J. (1989) Transfer function analysis of autonomic regulation. I. Canine atrial rate response. *Am J Physiol Heart Circ Physiol* 256, H142–H152.

Bibevski, S. & Dunlap, M.E. (1999) Ganglionic mechanisms contribute to diminished vagal control in heart failure. *Circulation* 99, 2958–2963.

Cerutti, C., Gustin, M.P., Paultre, C.Z., Lo, M., Julien, C., Vincent, M. & Sassard, J. (1991) Autonomic nervous system and cardiovascular variability in rats: a spectral analysis approach. *Am J Physiol Heart Circ Physiol* 261, H1292–H1299.

Du, X.J., Cox, H.S., Dart, A.M. & Esler, M.D. (1998) Depression of efferent parasympathetic control of heart rate in rats with myocardial infarction: effect of losartan. *J Cardiovasc Pharmacol* 31, 937–944.

Glantz, S.A. & Slinker, B.K. 2001. *Primer of Applied Regression & Analysis of Variance*, 2nd edn. McGraw-Hill, New York.

Kawada, T., Ikeda, Y., Sugimachi, M., Shishido, T., Kawaguchi, O., Yamazaki, T., Alexander, J. Jr. & Sunagawa, K. (1996) Bidirectional augmentation of heart rate regulation by autonomic nervous system in rabbits. *Am J Physiol Heart Circ Physiol* 271, H288–H295.

Kawada, T., Yamazaki, T., Akiyama, T., Li, M., Zheng, C., Shishido, T., Mori, H. & Sugimachi, M. (2007) Angiotensin II attenuates myocardial interstitial acetylcholine release in response to vagal stimulation. *Am J Physiol Heart Circ Physiol* 293, H2516–H2522.

Kawada, T., Mizuno, M., Shimizu, S., Uemura, K., Kamiya, A. & Sugimachi, M. (2009) Angiotensin II disproportionally attenuates dynamic vagal and sympathetic heart rate controls. *Am J Physiol Heart Circ Physiol* 296, H1666–H1674.

Kawada, T., Li, M., Kamiya, A., Shimizu, S., Uemura, K., Yamamoto, H. & Sugimachi, M. (2010) Open-loop dynamic and static characteristics of the carotid sinus baroreflex in rats with chronic heart failure after myocardial infarction. *J Physiol Sci* 60, 283–298.

Kawada, T., Uemura, K., Shimizu, S., Kamiya, A., Turner, M., Mizuno, M., Sunagawa, K. & Sugimachi, M. (2012) Consideration on parameter determination on a new model describing dynamic vagal heart rate control in rats. *Conf Proc IEEE Eng Med Biol Soc* 2012, 3809–3812.

Koumi, S., Arentzen, C.E., Backer, C.L. & Wasserstrom, J.A. (1994) Alterations in muscarinic K^+ channel response to acetylcholine and to G protein-mediated activation in atrial myocytes isolated from failing human hearts. *Circulation* 90, 2213–2224.

Levy, M.N. (1971) Sympathetic-parasympathetic interactions in the heart. *Circ Res* 29, 437–445.

Li, M., Zheng, C., Sato, T., Kawada, T., Sugimachi, M. & Sunagawa, K. (2004) Vagal nerve stimulation markedly improves long-term survival after chronic heart failure in rats. *Circulation* 109, 120–124.

Miyamoto, T., Kawada, T., Yanagiya, Y., Inagaki, M., Takaki, H., Sugimachi, M. & Sunagawa, K. (2004) Cardiac sympathetic nerve stimulation does not attenuate dynamic vagal control of heart rate via alpha-adrenergic mechanism. *Am J Physiol Heart Circ Physiol* 287, H860–H865.

Mizuno, M., Kamiya, A., Kawada, T., Miyamoto, T., Shimizu, S. & Sugimachi, M. (2007) Muscarinic potassium channels augment dynamic and static heart rate responses to vagal stimulation. *Am J Physiol Heart Circ Physiol* 293, H1564–H1570.

Mizuno, M., Kawada, T., Kamiya, A., Miyamoto, T., Shimizu, S., Shishido, T., Smith, S.A. & Sugimachi, M. (2010) Dynamic characteristics of heart rate control by the autonomic nervous system in rats. *Exp Physiol* 95, 919–925.

Mizuno, M., Kawada, T., Kamiya, A., Miyamoto, T., Shimizu, S., Shishido, T., Smith, S.A. & Sugimachi, M. (2011) Exercise training augments the dynamic heart rate response to vagal but not sympathetic stimulation in rats. *Am J Physiol Regul Integr Comp Physiol* 300, R969–R977.

Nakahara, T., Kawada, T., Sugimachi, M., Miyano, H., Sato, T., Shishido, T., Yoshimura, R., Miyashita, H., Inagaki, M., Alexander, J. Jr. & Sunagawa, K. (1998) Accumulation of cAMP augments dynamic vagal control of heart rate. *Am J Physiol* 275, H562–H567.

Olshansky, B., Sabbah, H.N., Hauptman, P.J. & Colucci, W.S. (2008) Parasympathetic nervous system and heart failure: pathophysiology and potential implications for therapy. *Circulation* 118, 863–871.

Persson, P.B. & Henriksson, J. (2011) Good publication practise in physiology. *Acta Physiol* 203, 403–407.

Riegger, A.J. (1985) Neurohumoral vasoconstrictor systems in heart failure. *Eur Heart J* 6, 479–489.

Sagawa, K. 1983. Baroreflex control of systemic arterial pressure and vascular bed. In: J.T. Shepherd & F.M. Abboud, (eds) *Handbook of Physiology, Sect 2, The Cardiovascular System, Vol III, Peripheral Circulation and Organ Blood Flow*, pp. 453–496. Am Physiol Soc, Bethesda, MD.

Sato, T., Kawada, T., Miyano, H., Shishido, T., Inagaki, M., Yoshimura, R., Tatewaki, T., Sugimachi, M., Alexander, J. Jr. & Sunagawa, K. (1999) New simple methods for isolating baroreceptor regions of carotid sinus and aortic depressor nerves in rats. *Am J Physiol Heart Circ Physiol* 276, H326–H332.

Schwartz, P.J. (2011) Vagal stimulation for heart diseases: from animals to men. – An example of translational cardiology. *Circ J* 75, 20–27.

Shoukas, A.A., Callahan, C.A., Lash, J.M. & Haase, E.B. (1991) New technique to completely isolate carotid sinus baroreceptor regions in rats. *Am J Physiol Heart Circ Physiol* 260, H300–H303.

Task Force of the European Society of Cardiology, the North American Society of Pacing and Electrophysiology (1996) Heart rate variability: standards of measurement, physiological interpretation and clinical use. *Circulation* 93, 1043–1065.

Wetzel, G.T., Goldstein, D. & Brown, J.H. (1985) Acetylcholine release from rat atria can be regulated through an α_1-adrenergic receptor. *Circ Res* 56, 763–766.

Appendix A mathematical model for the transfer function from VNS to HR in rats

The newly proposed transfer function model has a degree of freedom sufficient to describe the transfer function from VNS to HR observed in the present study. The fitting was performed in the frequency domain to minimize the following error function (Kawada *et al.* 2012).

$$\mathrm{err} = \sum_{k=1}^{N} \frac{1}{k} |\log[H(f_k)] - \log[M(f_k)]|^2$$

$$f_k = f_0 \times k$$

where log indicates a complex logarithmic function, f_0 is the fundamental frequency of the Fourier transformation, k is the index of frequency, and f_k is the k-th frequency. $H(f_k)$ and $M(f_k)$ are the estimated and model transfer functions respectively. This error function allows simultaneous approximation of gain and phase. N indicates the number of data points to fit and was set to 102 to approximate the transfer function up to 1 Hz.

J Pharmacol Sci 121, 1 – 8 (2013)

Journal of Pharmacological Sciences

Full Paper

Effects of an hERG Activator, ICA-105574, on Electrophysiological Properties of Canine Hearts

Mahoko Asayama[1,2], Junko Kurokawa[1,*], Kiyoshi Shirakawa[2], Hisashi Okuyama[2], Toshiki Kagawa[2], Jun-ichi Okada[3], Seiryo Sugiura[3], Toshiaki Hisada[3], and Tetsushi Furukawa[1]

[1]*Department of Bio-informational Pharmacology, Medical Research Institute, Tokyo Medical and Dental University, 1-5-45 Yushima, Bunkyo-ku, Tokyo 113-8510, Japan*

[2]*Safety Evaluation Research Laboratories, Research Division, Mitsubishi Tanabe Pharma Corporation, Tokyo 103-8405, Japan*

[3]*Graduate School of Frontier Sciences, the University of Tokyo, Chiba 277-8563, Japan*

Received October 3, 2012; Accepted October 29, 2012

Abstract. In short QT syndrome, inherited gain-of-function mutations in the human *ether a-go-go-related* gene (hERG) K^+ channel have been associated with development of fatal arrhythmias. This implies that drugs that activate hERG as a side effect may likewise pose significant arrhythmia risk. hERG activators have been found to have diverse mechanisms of activation, which may reflect their distinct binding sites. Recently, the new hERG activator ICA-105574 was introduced, which disables inactivation of the hERG channel with very high potency. We explored characteristics of this new drug in several experimental models. Patch clamp experiments were used to verify activation of hERG channels by ICA-105574 in human embryonic kidney cells stably-expressing hERG channels. ICA-105574 significantly shortened QT and QTc intervals and monophasic action potential duration (MAP_{90}) in Langendorff-perfused guinea-pig hearts. We also administered ICA-105574 to anesthetized dogs while recording ECG and drug plasma concentrations. ICA-105574 (10 mg/kg) significantly shortened QT and QTc intervals, with a free plasma concentration of approximately 1.7 μM at the point of maximal effect. Our data showed that unbound ICA-105574 caused QT shortening in dogs at concentrations comparable to the half maximal effective concentration (EC_{50}, 0.42 μM) of hERG activation in the patch clamp studies.

Keywords: hERG activator, QT and QTc interval, KCNH2, I_{Kr} channel, pro-arrhythmia

Introduction

The rapid delayed rectifier K^+ channel current (I_{Kr}) conducted by the human *ether a-go-go-related* gene (hERG, now termed KCNH2) channel is a major contributor to repolarization of the cardiac action potential (1). Loss-of-function mutations in hERG are associated with long QT syndrome (type LQT-2), which is a syndrome characterized by prolonged QT intervals on the electrocardiogram (ECG) and a ventricular tachycardia called torsades de pointes (TdP) (1, 2). There is an acquired form of long QT syndrome typically caused by blockade of I_{Kr} by commonly prescribed drugs, which can result in serious consequences including lethal arrhythmias and/or cardiac sudden death (3). In contrast, little is known about the consequences of enhanced activation of the hERG channel, whether induced by genetic mutations or by pharmacological intervention. A form of inherited short QT syndrome (SQT-1) associated with a gain-of-function mutation in the hERG channel was first reported in 2004 (4). At the cellular and tissue level, hERG activators have been employed to simulate SQT-1 and explore the cellular basis for its arrhythmogenesis. Based on structure–action-relationship analysis of hERG channels, previous hERG activators can be classified into at least two types. The drug RPR260243 binds to residues located near the intracellular end of the S5 and S6 transmembrane segments of the hERG channel and augments I_{Kr} currents by a dual mechanism of slowed deactivation and attenuated P-type inactivation. Alternatively, PD-

*Corresponding author. junkokuro.bip@mri.tmd.ac.jp
Published online in J-STAGE on December 14, 2012 (in advance)
doi: 10.1254/jphs.12220FP